University of Central Florida
STARS

Electronic Theses and Dissertations | Doctoral Dissertation (Open Access)

Amyotrophic Lateral Sclerosis: mechanism behind mutant SOD toxicity and improving current therapeutic strategies

2014

Cassandra Dennys
University of Central Florida

Find similar works at: https://stars.library.ucf.edu/etd

University of Central Florida Libraries http://library.ucf.edu

 Part of the Neuroscience and Neurobiology Commons

STARS Citation

Dennys, Cassandra, "Amyotrophic Lateral Sclerosis: mechanism behind mutant SOD toxicity and improving current therapeutic strategies" (2014). *Electronic Theses and Dissertations*. 1213.
https://stars.library.ucf.edu/etd/1213

This Doctoral Dissertation (Open Access) is brought to you for free and open access by STARS. It has been accepted for inclusion in Electronic Theses and Dissertations by an authorized administrator of STARS. For more information, please contact lee.dotson@ucf.edu.

AMYOTROPHIC LATERAL SCLEROSIS: MECHANISM BEHIND MUTANT SOD TOXICITY AND IMPROVING CURRENT THERAPEUTIC STRATEGIES

by

CASSANDRA N. DENNYS
B.Sc., Trent University, 2008
M.Sc., University of Central Florida, 2013

A dissertation submitted in partial fulfillment of the requirements
for the degree of Doctor of Philosophy in Biomedical Science
in the Burnett School of Biomedical Science
in the College of Medicine
at the University of Central Florida
Orlando, Florida

Summer
2015

Major Professor: Alvaro G. Estevez

© 2015 Cassandra N. Dennys

ABSTRACT

Amyotrophic Lateral Sclerosis (ALS) is an always lethal motor neuron disease with unknown pathogenesis. Inhibitors of the molecular chaperone heat shock protein 90 (Hsp90) have limited neuroprotection in some models of motor neuron degeneration. However the direct effect of Hsp90 inhibition on motor neurons is unknown. Here we show that Hsp90 inhibition induced motor neuron death through activation of the P2X7 receptor. Motor neuron death required phosphatase and tensein homolog (PTEN)-mediated inhibition of the PI3K/AKT pathway leading to Fas receptor activation and caspase dependent death. The relevance of Hsp90 for motor neuron survival was investigated in mutant Cu/Zn superoxide dismutase (SOD) transgenic animal models for ALS. Nitrated Hsp90, a posttranslational modification known to induce cell death (Franco, Ye et al. 2013), was present in motor neurons after intracellular release of zinc deficient (Zn, D83S) and the SOD in which copper binding site was genetically ablated (Q) but not after copper deficient (Cu) wild type SOD. Zn deficient and Q mutant SOD induced motor neuron death in a peroxynitrite mediated and copper dependent mechanism. Nitrated Hsp90 was not detected in the spinal cord of transgenic animals for ALS-mutant SOD animal models until disease onset. Increased nitrated Hsp90 concentrations correlated with disease progression. Addition of Zn or Q SOD to nontransgenic brain homogenate treated with peroxynitrite led to an increase level of nitrotyrosine in comparison to wild type controls. However, in the same samples there was a 2 to 10 time increase in Hsp90 nitration as compared to nitrotyrosine. The selective increase is likely due to the binding of Hsp90 to Zn deficient and Q SOD as

oppose to wild type SOD. These results suggest that Hsp90 nitration facilitated by mutant SOD may cause motor neuron degeneration in ALS. Targeted inhibition of nitrated Hsp90 may be a novel therapeutic approach for ALS. An alternative therapeutic strategy is to target the production of survival factors by glial cells. Riluzole is the only FDA approved drug for the treatment of ALS and it shows a small but significant increase in patient lifespan. Our results show that acute riluzole treatment stimulated trophic factor production by astrocytes and Schwann cells. However long-term exposure reversed and even inhibited the production of trophic factors, an observation that may explain the modest increase in patient survival in clinical trials. Discontinuous riluzole treatment can maintain elevated trophic factor levels and prevent trophic factor reduction in spinal cords of nontransgenic animals. These results suggest that discontinuous riluzole administration may improve ALS patient survival. In summary, we demonstrated that Hsp90 has an essential function in the regulation of motor neuron survival. We have also shown that Hsp90 was nitrated in the presence of mutant SOD and was present during symptom onset and increases as disease progresses, which may explain the toxic gain of function of mutant SOD. Finally we demonstrate a biphasic effect of riluzole on trophic factor production and propose changes in administration to improve effects in ALS patients.

In loving memory of JC, for his unwavering faith in my success.

ACKNOWLEDGMENTS

First and foremost, I would like to thank my mentor, Dr. Alvaro Estevez, for his guidance and mentorship over the last four years. I could not have accomplished the achievements I have made without his ongoing support and encouragement. He believed in my ability to overcome challenges, and was there to groom, cultivate and develop me both personally and professionally.

Thank you to my committee, especially Dr. Annette Khaled, for recognizing my potential, your unwavering advocacy, and for providing the support to achieve my goals. Thank you Dr. Cristina Fernandez-Valle, for the additional training provided by your lab in addition to your insightful knowledge and encouragement. I would also like to thank Dr. Kim, for his thought provoking questions which further enhanced my communication skills. Finally, thanks to Dr. Ebert for guiding me in the beginning years of my Ph.D.

I would also like to thank my role model, Dr. Maria Clara Franco, for her leadership and example. She always provided sound advice in relation to my career and professional development. Most importantly, she dedicated her time to nurturing a young scientist like myself and did so with a smile on her face.

Thank you to my lab mates who contributed both friendship and support over the years, especially, in no specific order, Kristen Thomas, JeNay Armstrong, Pascale Nelson, Megan Jandy, Catherine Mitchell, J. Andres Hernandez and Kristina Ramdial. As well as

our collaborators from Dr. Joseph Beckman's lab, Dr. Carol Milligan's lab, Dr. Cristina Fernandez Valle's lab, in addition to Marga Bott and Emiliano Trias, all of whom provided the expertise and materials necessary for project completion.

Finally I would like to thank my family for their ongoing support over the duration of my Ph.D, as well as my fiancé, Mike Rivers, for his understanding and support during my Ph.D career.

I would also like to thank our financial support from the NIH/NINDS and the university of Central Florida, as well Dr. Griffith Parks for all his support.

TABLE OF CONTENTS

LIST OF FIGURES

LIST OF TABLES

LIST OF SUPPLEMENTAL FIGURES

LIST OF ACRONYMS

AKT: protein kinase B

ALS: amyotrophic lateral sclerosis

apoSOD: metal deficient wild type SOD

BDNF: brain derived neurotrophic factor

CT-1: cardiotrophin-1

DAXX: death domain associated protein

FasL: Fas ligand, TNF subfamily, member 6

FasR: Fas cell surface death receptor

FADD: Fas associated protein death domain

FHRE: fork head responsive element

FOXO3a: forkhead box 03

GAPDH: Glyceraldehyde 3-phosphate dehydrogenase

GDNF: glial derived neurotrophic factor

HSF1: heat shock factor 1

Hsp40: heat shock protein 40

Hsp70: heat shock protein 70

Hsp90: heat shock protein 90

NGF: nerve growth factor

nNOS: neuronal nitric oxide synthase

NO_2Hsp90: nitrated Hsp90

NO_2Tyr: nitrotyrosine

PDK1: phosphoinositide-dependent kinase

PI3K: phophatidyl inositol-3 kinase

PIP2: phosphotidylinositol 4,5-bisphosphate

PIP3: phosphatidylinositol (3,4,5)-trisphosphate

PTEN: phosphatase and tensin homolog

SOD: superoxide dismutase

Q SOD: mutant SOD with copper binding site genetically ablated

Zn SOD: zinc deficient SOD (D83S)

Cu SOD: copper deficient SOD (wild type)

CHAPTER 1: GENERAL INTRODUCTION

Amyotrophic Lateral Sclerosis is an always-fatal neurodegenerative disease characterized by the loss of motor neurons in the motor cortex, brain stem and ventral spinal cord (Rossi, Franco et al. 2013). It affects 2-3 in 100,000 people, with an average lifespan of 2-5 years following diagnosis. Approximately 10% of ALS cases are hereditary, or familiar, with an unknown pathological cause. 20-30% of the familiar form of ALS is linked to mutations in the superoxide dismutase (SOD) gene (Rosen, Siddique et al. 1993; Wang, Sharma et al. 2008). The identification of mutation in the gene of SOD allowed for the development of early transgenic mouse and rat models of ALS (Berthod and Gros-Louis 2012).

The contribution of ALS-linked mutant SOD to disease onset and progression remains highly controversial. Animals expressing mutant SOD in neuronal (Jaarsma, Teuling et al. 2008) or glial cells develop the disease phenotype (Papadeas, Kraig et al. 2011). Genetic deletion of SOD does not lead to disease (Reaume AG 1996) while cell-specific SOD knockout either delays disease onset or slows disease progression (Clement, Nguyen et al. 2003). On the other hand, overexpression of wild type SOD has no effect, or accelerates disease progression (Bruijn, Houseweart et al. 1998; Deng, Shi et al. 2006). These seminal discoveries led to the hypothesis that mutant SOD contributes to ALS pathology by a toxic gain-of-function. However the mechanism behind mutant SOD toxicity is still unknown.

Disease progression in a G93A mutant SOD transgenic mouse model is well described. Muscular denervation of fast twitch muscle is detected by postnatal day 30 (p30) (Vinsant, Mansfield et al. 2013; Vinsant, Mansfield et al. 2013), but the animals are still considered asymptomatic by p60. At p60, SOD aggregates can be observed and there is some compromised motor function (Bruijn, Becher et al. 1997). During the early symptomatic stage (p90) there is extensive motor neuron death and dysfunction (Gurney, Pu et al. 1994; Bruijn, Becher et al. 1997). Astrocytes (Barbeito, Pehar et al. 2004) and microglia (Liao, Zhao et al. 2012) are activated and nitrated proteins (Casoni, Basso et al. 2005) are observed in both motor neurons and glial cells. By end stage (p120), massive motor neuron loss is observed, slow twitch muscle are denervated and the myelin sheath is compromised (Vinsant, Mansfield et al. 2013; Vinsant, Mansfield et al. 2013). *In vivo*, cell-specific SOD knockout in oligodendrocytes (Kang, Li et al. 2013), astrocytes (Yamanaka, Chun et al. 2008), and microglia slows disease progression where as neuronal specific knockout delays disease onset (Boillee, Yamanaka et al. 2006). *In vitro*, conditioned media and co-culture experiments utilizing astrocytes overexpressing mutant SOD is toxic to motor neurons (Nagai, Re et al. 2007; Basso, Pozzi et al. 2013; Re, Le Verche et al. 2014). This suggests a switch from secretion of pro-survival trophic factors to toxic factors from astrocytes. Importantly, delivery of mutant SOD to pure motor neurons cultured in the presence of trophic factors induces cell death in a peroxynitrite and copper dependent mechanism (Estévez, Crow et al. 1999; Sahawneh, Ricart et al. 2010). These findings reveal that both cell autonomous and non-cell autonomous mechanisms contribute to the pathology.

Riluzole is currently the only FDA approved drug for the treatment of ALS. Riluzole has been shown to slightly extend lifespan of mutant SOD transgenic mice and ALS patients. However, it only extends lifespan in patients for three months to one year (Bensimon, Lacomblez et al. 1994; Gurney, Cutting et al. 1996; Lacomblez, Bensimon et al. 1996; Lacomblez, Bensimon et al. 1996; Gurney, Fleck et al. 1998). Riluzole has been shown to stimulate glutamate reuptake, block sodium channels and stimulate trophic factor production by glial cells (Doble 1997; Peluffo, Estévez et al. 1997; Meininger, Lacomblez et al. 2000; Cheah, Vucic et al. 2010; Bellingham 2011; Dennys, Armstrong et al. 2015). The primary mechanism of action was thought to be by preventing glutamate toxicity, but the development of other antiglutamates had no effect on ALS patient survival (Miller, Moore et al. 2001). Consequently, the primary mechanism of action remains unknown. Understanding the primary therapeutic effect of riluzole in ALS may lead to the development of new drugs or enhanced effectiveness of current therapies.

The unknown underlying cause of ALS limits the development of therapeutically effective treatments. This dissertation aims to advance the field of ALS in three ways:

1. Identify critical molecular targets in the regulation of motor neuron survival
2. Identify toxic gain of function of mutant SOD
3. Improve effectiveness of current therapeutic strategies and identify novel therapeutic targets

CHAPTER 2: HSP90 IS CRITICAL FOR MOTOR NEURON SURVIVAL

Introduction

Heat shock protein (Hsp90) is a ubiquitous molecular chaperone that totals approximately 1-2% of cytosolic proteins (Didelot, Schmitt et al. 2006). Hsp90 participates in the regulation of a variety of pro-survival cellular processes through interactions with more than 200 client proteins, including numerous transcription factors and kinases such as phosphatidyl inositol-3 kinase (PI3K), phosphoinositide-dependent kinase-1 (PDK1) and Akt (Pearl and Prodromou 2000; Richter and Buchner 2001; Picard 2002; Pratt and Toft 2003; Whitesell and Lindquist 2005; Zhao, Davey et al. 2005; Gaestel 2006; Pearl and Prodromou 2006; Pratt, Morishima et al. 2008; Mollapour and Neckers 2011; Li and Buchner 2013). In most cells, alteration of the interaction of Hsp90 with the transcription factor heat shock factor 1 (HSF1) results in the expression of stress proteins such as heat shock protein 70 and 40 (Hsp70 and Hsp40) (Richter, Haslbeck et al. 2010; Robinson, Gifondorwa et al. 2010). However, motor neurons do not have a typical stress response and fail to induce the expression of Hsp70 (Newbern, Taylor et al. 2005), a condition that is reversed by HSF1 overexpression (Batulan, Taylor et al. 2006). These results suggest that motor neurons have a higher threshold for the induction of the heat shock response (Batulan, Shinder et al. 2003; Batulan, Taylor et al. 2006). In contrast, in the same

conditions astrocytes induce and release Hsp70, which is a survival factor for motor neurons (Robinson, Tidwell et al. 2005; Taylor, Gifondorwa et al. 2007).

The benzoquinone ansamycin antibiotic geldanamycin, is a specific inhibitor of Hsp90 that binds to the unusual ATPase binding site within the N-terminus domain of the chaperone inhibiting its ATPase activity (Prodromou, Roe et al. 1997; Stebbins, Russo et al. 1997). Inhibition of Hsp90 using geldanamycin in dissociated spinal cord cultures stimulates the expression of Hsp40 and Hsp70 by motor neurons and prevents mutant SOD-dependent motor neuron death (Batulan, Taylor et al. 2006). Hsp90 inhibition prevents also glutamate toxicity in a mouse hippocampal cell line (Xiao, Callaway et al. 1999). However, inhibition of Hsp90 also activates the heat shock response in astrocytes, leading to the release of Hsp70 and subsequent uptake by motor neurons, which improves motor neuron survival (Taylor, Gifondorwa et al. 2007). Therefore it remains to be determined whether the protection afforded by Hsp90 inhibitors is due to direct effects on motor neurons. Here, we investigated the direct effects of Hsp90 inhibition on purified motor neurons cultures. Pure motor neurons were 10-1000 times more susceptible to inhibition of Hsp90 by geldanamycin than any other cell type tested. Inhibition of Hsp90 triggered motor neuron death by the P2X7 receptor-dependent activation of PTEN, leading to inhibition of the pro-survival PI3K/Akt pathway and activation of the Fas death pathway.

Materials and Methods

Motor neuron cell culture: Motor neurons were prepared as previously described (Henderson, Bloch-Gallego et al. 1995; Raoul, Henderson et al. 1999; Franco, Ye et al. 2013). Briefly, isolated ventral spinal cords from E15 rat embryos were trypsinized and the tissue disaggregated by trituration. The cell suspension was centrifuged on top of a 6% OptiPrep cushion (Sigma, Saint Louis, MO) and the motor neurons were removed from the interface. Motor neurons were further purified by magnet-assisted cell separation (Miltenyi Biotec, Auburn CA) using an antibody against p75 low-affinity neurotrophin receptor (Chemicon-Milliport, Billerica, MA). Motor neurons were plated on 96 well plates (750 cells per well), 35 mm plates (20,000 cells per plate, with the exception of 100,000 cells per plate for western blots for FOXO3a), 4-well plates (3,000 cells per well), or 8-well chamber slides (30,000 cells per well) coated with poly-DL-ornithine and laminin (Sigma). Motor neurons were maintained in neurobasal media supplemented with B27, heat inactivated horse serum, glutamine, glutamate, 3-mercaptoethanol (all from Gibco/Invitrogen, Carlsbad, CA) and trophic factors (1 ng/ml BDNF, 0.1 ng/ml GDNF, 10 ng/ml cardiotrophin-1), and incubated in a 5% CO_2 humidified atmosphere at 37°C.

Cortical neuron cell culture: Cortical neurons were obtained from the cerebral cortex of fetal Sprague Dawley rats (E17) by a papain dissociation method as described previously (Gonzalez-Zulueta, Ensz et al. 1998). Cultures were plated on poly-D-lysine (Sigma-

Aldrich)-coated cell culture dishes and maintained in minimum essential medium (MEM) (Invitrogen, Grand Island, NY) containing 5.5 g/L glucose, 2 mM glutamine, 100 μM cystine, and supplemented with 10% fetal bovine serum (FBS; Invitrogen) and 1% penicillin/streptomycin (Invitrogen). Cultures plated at a low density (10,000 cells/ml) were maintained in MEM containing 10% horse serum (HS; Invitrogen) instead of FBS and 10 μM BHA (Invitrogen). All experiments were initiated 24 h after plating.

NSC34 cell culture: NSC34 motor neuron hybrid line was maintained in DMEM containing 10% FBS and 1% Penicillin/Streptomycin at 37◦C during the growth stage. To differentiate the cells, 10% HS was substituted for FBS and 1 μM retinoic acid was added. The cells were differentiated for a period of one week prior to treatments.

Motor neuron survival: Motor neuron survival was determined either by counting by hand in four well plates (Nunc) or by calcein staining (Molecular Probes, Invitrogen) for 45 minutes in black 96-well plates (Greiner Bio-One, Monroe, NC) as previously described (Franco, Ye et al. 2013). Extracellular calcein was quenched with 100 mg/mL hemoglobin and the images were captured using the RUNNER (Trophos, Marseilles, France). Cell counts were obtained using the Tina software (Trophos). Cell counts are represented as percent survival relative to the survival of neurons in the presence of neurotrophic factors alone.

Immunofluorescence: Motor neurons were plated in 4-well chamber slides and fixed in paraformaldehyde and processed for immunofluorescence (Franco, Ye et al. 2013). Cells were briefly prefixed with 4% paraformaldehyde (PFA) and 0.1% glutaraldehyde in same volume of original media for 2 minutes on ice. Cells were rinsed 3 times with PBS containing magnesium and calcium and incubated for 20 minutes with 4% PFA and 0.1% glutaldehyde. Cells were then incubated with anti-mouse in 4% goat serum for 1 hr to block the purification antibody and fixed with 4% PFA and 0.1% glutaldehyde for 15 minutes. After rinsing with PBS, cells were incubated with 50 mM glycine and 0.2% Triton X-100 in PBS for 30 minutes at room temperature. Cells were then incubated with signal enhancer (Invitrogen) for 30 minutes room temperature. Cells were blocked using 4% goat serum and 0.2% Triton X-100 at room temperature for 1 hour. Primary antibodies, FoxO3a (Cell Signaling) and MAP2 (Sigma) were incubated in blocking solution in a humidified chamber at 4°C overnight and then rinsed 3 times with PBS. Cells were incubated with fluorescent secondary antibodies [AlexaFluor 594 donkey anti-mouse IgG and AlexaFluor 488 donkey anti-rabbit (Invitrogen)] for 1 hour at room temperature protected from light. Cells were then stained with DAPI and rinsed three times with PBS and once with water once before being mounted using ProLong Gold (Molecular Probes, Invitrogen, Eugene, OR).

Microscopy: Immunoflourescence was imaged using Carl Zeiss Observer A1 with AxioVision 2010 acquisition software. All images were taken using a Zeiss oil immersion, 63X/1.40 Plan Apochromat objective (#420781-9910). Image acquisition for

each channel (exposure, brightness, contrast and gamma) was taken at the same settings for each image. Brightness was adjusted in the Zen software post-acquisition to produce the best image possible and was set to the same levels across experimental groups.

Immunoblotting: Cells were lysed using a NP-40 lysis buffer (1% NP-40, 40 mM Tris, pH 7.4, 0.15 M NaCl, 10% glycerol, 0.1% SDS, 0.1% deoxycholate) or RIPA buffer (25mM Tris-HCl (pH 7.6), 150mM NaCl, 1% NP-40, 1% sodium deoxycholate, 0.1% SDS) containing protease and phosphatase inhibitors. Cells were subjected to sonication or freeze-thaw and then centrifuged to collect supernatant. Lysate was separated by SDS-PAGE before transfer to PVDF membrane. After blocking with Odyssey Blocking Buffer (LI-COR Biosciences), membranes were incubated with primary antibodies overnight at 4°C, washed, incubated with secondary antibodies for 1 h at room temperature, washed, and scanned. The LI-COR Biosciences Odyssey Infrared Imaging system was used to visualize blots. Secondary antibodies were obtained from LI-COR Biosciences (IR 680 goat anti-rabbit IgG and IR 800 goat-anti-mouse IgG or 680 donkey anti-rabbit and 700 donkey anti goat). Primary antibodies were the following: Akt, pAkt (Ser473), pAKT (thr308), FoxO3a, pPDK1 (Ser 241) and Myc from Cell Signaling, FasL (N-20) from Santa Cruz, and PDK1 from BD Biosciences. Bands were quantified using ImageJ software.

Quantitative RT-PCR: RNA was extracted and purified using the Trizol-based PureLink RNA kit (Invitrogen). The cDNA was synthesized using SuperScript First-Strand

Synthesis (Invitrogen). Real-time PCR was performed using the 7500 Fast Real-Time PCR System and SDS software (Applied Biosystems). TaqMan Fast Universal PCR Mix and TaqMan fluorescent probes for Fas ligand, Fas receptor, GAPDH, and β-actin were obtained from Applied Biosystems.

Adenoviral vectors construction: The p110-CAAX subunit of PI3K, A280V PDK1 and N-term myristolyation AKT1 were cloned separately into pAdTrack-CMV using restriction enzymes SalI and EcoRV (Genscript Corporation, Piscataway, NJ). The adenoviral vectors were prepared and amplified as previously described (He, Zhou et al. 1998). Briefly, the linear vectors were electroporated in chemically competent cells containing pAdEasy1. The resulting adenoviral vector co-expressing GFP was digested with *Pac1* and transfected into HEK293A cells using Lipofectamine 2000 (Invitrogen). The infected cells were cultured until all cells were GFP positive, at which time cells were lifted and lysed by freeze/thaw. The viral stock was then amplified to a titer of $1x10^{-8}$.

Motor neuron transduction: Purified motor neurons (80 motor neurons/μl) were incubated with the adenoviral vectors at a multiplicity of infection of 120 for 2 hours at 4°C in transduction media (1% heat inactivated fetal bovine serum, 20 μM glucose, 0.5 μg/mL insulin, 10 μM putrescine, 10 μg/mL conalbumin, and 0.3 nM sodium selenite, 20 nM progesterone). Motor neurons were then plated at a density of 3,000 cells/well in a 4 well plate and cultured for 72 h at 37°C, 5% CO_2/air prior to experimentation.

Luciferase assay: Motor neurons were plated for 2 hours before being transduced (MOI 160) with a lentivirus producing luciferase under the control of the forkhead responsive element (Qiagen). The following day, motor neurons were treated with 0.5 nM geldanamycin for 16 hours. Cells were lysed with the Promega One-Glo luciferase kit and luminescence was measured on a microplate reader for 10 seconds.

Statistical analysis: Graphing and statistical analysis was performed using Prism software (Graphpad). Multiple comparisons were performed using one or two-way ANOVA, followed by the Bonferroni multiple comparison test or student T-test. Survival and dose response data were fit to a sigmoidal curve. Values were considered significantly different when $p < 0.05$. All experiments were performed in triplicate.

Results

Motor neurons are highly sensitive to inhibition of Hsp90. The effect of Hsp90 inhibition on motor neuron survival was assessed in pure motor neuron cultures incubated with increasing concentrations of the Hsp90 inhibitor geldanamycin and in the presence or absence of trophic factors. Motor neurons cultured in the presence of trophic factors with geldanamycin for 24 h were 10 times more sensitive to Hsp90 inhibition than the motor neurons that survived without trophic factors and incubated with geldanamycin for 24 h (Fig. 1A and B). The sensitivity of pure motor neurons to Hsp90 inhibition was investigated by comparing the EC_{50} of geldanamycin-induced motor neuron death to that

of cultures of dissociated embryo ventral spinal cord and cortical neurons at low and high density (Fig. 1C and D), and undifferentiated and differentiated cultures of the hybrid motor neuron cell line NCS34 (Fig. 1E). The EC_{50} of purified motor neurons cultured in the presence of trophic factors was between 10-10,000 times lower than the equivalent value for all other cell types (Table 1). This sensitivity was not due to variations in overall levels of Hsp90 in motor neurons (Fig. 1F and G). Thus, inhibition of Hsp90 induces motor neuron death and the vulnerability of motor neurons to Hsp90 inhibition is enhanced by activation of trophic signaling pathways. These results suggest that motor neurons are more sensitive to inhibition of Hsp90 due to activation of a specific cell death-signaling pathway not present in other cell types or because motor neurons are more sensitive to the inhibition of a critical pro-survival pathway.

Inhibition of Hsp90 activates the Fas receptor/FasL pathway. Motor neurons cultured in the presence of trophic factors were an order of magnitude more sensitive to inhibition of Hsp90 than motor neurons deprived of trophic factors (Table 1), suggesting that inhibition of Hsp90 may activate the same cell death pathway induced by trophic factor deprivation. Trophic factor deprivation leads to the activation of the Fas pathway and subsequent motor neuron apoptosis (Raoul, Henderson et al. 1999; Raoul, Estévez et al. 2002). Indeed, incubation of motor neurons with 0.5 nM geldanamycin in the presence of the Fas ligand (FasL) decoy Fas:FC completely prevented motor neuron death (Fig. 2A). However, Fas:Fc only shifted the EC_{50} for geldanamycin toxicity to values comparable to those of trophic factor deprivation (EC_{50}: 4.8 nM, 95% CI: 3.5 nM to 6.5 nM, Fig. 2B).

This observation reveals the existence of a Fas-independent cell death pathway triggered at higher concentrations of geldanamycin were Fas:FC is only partially protective. Transcription and translation of FasL is necessary for the activation of Fas-mediated apoptosis in trophic factor deprived motor neurons or motor neuron carrying amyotrophic lateral sclerosis (ALS)-linking mutant superoxide dismutase (SOD) in the presence of nitric oxide (Raoul, Henderson et al. 1999; Raoul, Estévez et al. 2002). Inhibition of both transcription and translation prevented geldanamycin-induced apoptosis (Fig. 2C), suggesting that geldanamycin-induced motor neuron death required *de novo* protein synthesis. Indeed, the expression of the FasL messenger RNA was stimulated 18 h after Hsp90 inhibition (Fig. 2D), without affecting the expression of Fas receptor (Fig. 2E). These results suggest that in the presence of trophic factors, Hsp90 activity is essential to motor neuron survival.

In motor neurons, stimulation of the DAXX component of the Fas pathway leads to activation of p38-MAP kinase, expression of neuronal nitric oxide synthase (nNOS) and production of peroxynitrite (Raoul, Estévez et al. 2002). To investigate the role of the DAXX component of the Fas pathways in the induction of apoptosis, motor neurons were incubated with geldanamycin and the NOS inhibitor, L-NAME. Inhibition of NOS did not prevent geldanamycin-induced motor neuron death, but it did prevent cell death stimulated by trophic factor deprivation (Fig. 3A). Production of 80-120 nM steady state concentrations of nitric oxide did not affect geldanamycin-induced motor neuron death (Fig. 3B). Similarly, incubation of motor neurons with 0.5 nM geldanamycin in the

presence of the SOD mimetic, MnTBAP, and the superoxide and peroxynitrite scavenger, FeTCPP, did not prevent motor neuron death. However, MnTBAP and FeTCPP at the same concentrations prevented apoptosis induced by trophic factor deprivation (Fig. 3C). Inhibition of p38 also failed to prevent motor neuron death induced by inhibition of Hsp90 (Fig. 3D). Motor neuron death downstream of Fas receptor activation may also occur independently of peroxynitrite production by stimulation of the FADD component of the Fas pathway involving the activation of caspases (Raoul, Estévez et al. 2002; Franco, Ye et al. 2013). Indeed, the pan caspase inhibitor z-VAD and selective inhibitors for caspases 3, 8, and 9 prevented geldanamycin-induced motor neuron death (Fig. 2F). Together, these results reveal that inhibition of Hsp90 stimulates motor neuron apoptosis by a Fas-dependent and peroxynitrite-independent mechanism.

Hsp90 inhibition induces FOXO3a dependent transcription. FasL expression in motor neurons is mediated by the activation of forkhead box 03 (FOXO3a) (Barthelemy, Henderson et al. 2004). Activation of FOXO3a is stimulated by dephosphorylation of ser253 (Brunet, Bonni et al. 1999; Tang, Nunez et al. 1999). Incubation of motor neurons with geldanamycin reduced the phosphorylation levels of FOXO3a, with no change in total levels of the transcription factor (Fig 4A-C). Consequently, FOXO3a translocated to the nucleus after inhibition of Hsp90 (Fig. 4D). The activity of FOXO3a was measured by transducing motor neurons with a reporter construct carrying luciferase under the control of the forkhead responsive element (FHRE). There was a two fold increase in the luciferase activity of motor neurons incubated with geldanamycin for 16 h

compared to untreated controls (Fig. 4E). No changes in cell number were detected after 16 h incubation with geldanamycin (Fig. 4F), revealing that inhibition of Hsp90 activates FOXO3a-dependent transcription.

Hsp90 inhibition leads to PTEN-mediated inhibition of the PI3K/Akt pathway upstream of Fas receptor activation. Inhibition of the PI3K pathway leads to translocation of FOXO3a to the nucleus (Mojsilovic-Petrovic, Nedelsky et al. 2009). Downstream of PI3K, PDK1 and Akt are Hsp90 clients (Sato, Fujita et al. 2000; Basso, Solit et al. 2002; Fujita, Sato et al. 2002). To investigate whether inhibition of the PI3K pathway led to the induction of Fas-dependent apoptosis, motor neurons were incubated with the PI3K inhibitors LY294002 and wortmannin in the presence or absence of Fas:Fc and in the presence of trophic factors. Fas:Fc prevented LY294002 and wortmannin-induced motor neuron death (Fig. 5), suggesting that in the presence of trophic factors, activation of the PI3K pathway prevents Fas-induced motor neuron death. Incubation of motor neurons with geldanamycin reduced phosphorylation of Akt at Ser 473 after 18 and 24 hours (Fig. 6A) with a smaller but faster decrease in phosphorylation at Thr 308 (Fig. 6B) and no change in total Akt (Fig. 6C). These results suggest that geldanamycin does not affect the formation of the complex Hsp90/Akt, which will result in a decrease in total Akt (Sato, Fujita et al. 2000). In addition, inhibition of Hsp90 did not affect PDK1 intracellular levels (Fig. 6D). Expression of constitutively active Akt1, PDK1, and PI3K in motor neurons using adenoviral vectors prevented geldanamycin-induced motor neuron death (Fig. 7A and B). These results suggest that inhibition of Hsp90 prevents the

activation of the PI3K/Akt pro-survival pathway upstream of PI3K activation, ultimately leading to activation of the Fas/FasL pathway.

The phosphatase and tensin homolog (PTEN) inhibits the PI3K/Akt pathway by dephosphorylating phosphatidyl-inositol,3,4,5 triphosphate (PIP3) to phosphatidylinositol-3,4-diphosphate (PIP2), thus preventing the activation of PDK1 (Weng, Brown et al. 2001; Jiang and Liu 2008). Pharmacological inhibition or down-regulation of PTEN prevented induction of motor neuron death by geldanamycin (Fig. 7C and 7D). These results reveal that stimulation of PTEN by inhibition of Hsp90 prevents activation of PDK1, decreasing Akt activity and triggering motor neuron death.

Hsp90 inhibition activates P2X7 receptor. Hsp90 is a negative regulator of the P2X7 ionotropic ATP-gated receptor (Adinolfi, Kim et al. 2003). Activation of P2X7 receptor stimulates an influx of calcium that triggers motor neuron death through the activation of the Fas pathway (Franco, Ye et al. 2013; Gandelman, Levy et al. 2013). Inhibition of the P2X7 receptor with brilliant blue G or down-regulation using siRNA prevented motor neuron death stimulated by Hsp90 inhibition. The intracellular calcium chelator BAPTA-AM also prevented motor neuron death stimulated by inhibition of Hsp90 (Fig. 8). To determine whether Hsp90 inhibition was derepressing P2X7 receptor or stimulating the release of ATP, motor neurons were incubated with geldanamycin in the presence of the ATP-degrading enzyme apyrase. Incubation with apyrase did not affect geldanamycin-

induced motor neuron death (Fig. 8), suggesting that inhibition of Hsp90 activates P2X7 receptor independently of its ligand ATP.

Discussion

P2X7 receptor stimulates motor neuron apoptosis by a Fas-dependent pathway (Franco, Ye et al. 2013; Gandelman, Levy et al. 2013). Furthermore, phosphorylated Hsp90 is a negative regulator of P2X7 receptor (Adinolfi, Kim et al. 2003). In agreement with a negative role on P2X7 receptor activation, motor neuron death induced by Hsp90 inhibition was prevented by both P2X7 receptor inhibition and down regulation of its expression. The Hsp90 associated to the P2X7 receptor complex seems to be very sensitive to inhibition by geldanamycin. Concentrations of geldanamycin in the picomolar range were sufficient to stimulated motor neuron death. In contrast, activation of the heat shock response in motor neurons requires higher concentrations of geldanamycin (Batulan, Shinder et al. 2003; Robinson, Tidwell et al. 2005). In fact motor neurons have an atypical heat shock response (Batulan, Shinder et al. 2003; Robinson, Tidwell et al. 2005). In normal conditions, HSF1 is kept in the cytoplasm by a complex that includes Hsp90 and Hsp70 (Richter, Haslbeck et al. 2010; Robinson, Gifondorwa et al. 2010). As a consequence of protein unfolding or inhibition of Hsp90 the complex dissociates releasing HSF1, which migrates to the nucleus and activates the expression of proteins associate with the stress response (Richter, Haslbeck et al. 2010; Robinson, Gifondorwa et al. 2010). Motor neurons have a high threshold for the

activation of the HSF1, which leads to a deficient stress response (Batulan, Shinder et al. 2003; Batulan, Taylor et al. 2006; Robinson, Gifondorwa et al. 2010). We found that highly purified motor neuron cultures incubated with trophic factors are abnormally sensitive to Hsp90 inhibition. The high sensitivity was not due to differential expression of Hsp90 respect to other cell types or tissues, but rather it seems to be characteristic of motor neurons. The affinity of geldanamycin and ATP for Hsp90 depends on post-translational modifications and the interaction with client proteins and co-chaperones (Fiskus, Rao et al. 2008; Rao, Fiskus et al. 2008; Mahalingam, Swords et al. 2009; Walton-Diaz, Khan et al. 2013). Post-translational modifications and co-chaperons affect also the affinity of Hsp90 for client proteins (Pearl and Prodromou 2006; Mollapour, Tsutsumi et al. 2010; Li and Buchner 2013; Walton-Diaz, Khan et al. 2013). The combination of post-translational modifications and protein interactions of Hsp90 in the P2X7 complex in motor neurons may provide the conditions that make the chaperone exceptionally sensitive to geldanamycin inhibition. It is also possible that the same conditions that conferred a high threshold for the activation of the stress response are responsible for the high sensitivity to Hsp90 inhibition in motor neurons. However, there are clear differences on the effects of geldanamycin previously reported and our results, which can be explained by the different condition used to culture the motor neurons. The presence of other cells like astrocytes in the culture can mask direct effects of Hsp90 inhibition on motor neurons (Robinson, Tidwell et al. 2005; Robinson, Gifondorwa et al. 2010).

Motor neurons are highly dependent on the supply of trophic factors for survival both in culture and in vivo (Sendtner, Arakawa et al. 1991; Oppenheim, Yin et al. 1992; Henderson, Camu et al. 1993). The protection provide by trophic factors is due to activation of the PI3K/Akt pathway. Indeed, motor neurons are highly dependent on the activity of the PI3K/Akt pathway and inhibition of this pathway stimulates death by apoptosis (Milligan, Prevette et al. 1995; Li, Prevette et al. 1998; Dolcet, Egea et al. 1999; Raoul, Henderson et al. 1999; Soler, Dolcet et al. 1999; Garces, Haase et al. 2000). PDK1 and Akt are known clients of Hsp90. Hsp90 has the double function of preventing the degradation of the activated kinase, and through the binding of co-chaperones participates in directing the kinases to their targets (Basso, Solit et al. 2002; Fujita, Sato et al. 2002). Inhibition of Hsp90 in motor neurons down-regulated the PI3K/Akt pathway as determined by decreased Akt phosphorylation (Fig 6). Consistent with this interpretation, overexpression of constitutive active PDK1 and Akt prevented motor neuron death induced by inhibition of Hsp90. However, overexpression of the p110 constitutive active catalytic subunit of the PI3K also prevented motor neuron apoptosis induced by inhibition of Hsp90 (Fig. 7). To the best of our knowledge, PI3K is not a client of Hsp90, suggesting that Hsp90 inhibition is acting upstream of this kinase. Inhibition of PTEN, a well-known down regulator of the PI3K/Akt pathway has recently been shown to improve motor neuron survival and function in cell culture and *in vivo* models of motor neuron degeneration (Ning, Drepper et al. 2010; Kirby, Ning et al. 2011; Yang, Wang et al. 2014). PTEN inhibits PDK1 activation by catalyzing the dephosphorylation of phosphatidylinositol 3,4,5 triphostate (PIP3) to phosphatidylinositol

3,4 biphosphate (PIP2) (Fig. 9). Low levels of PIP3 prevent the activation of PDK1, inhibiting the activation of Akt and its down-stream cell signaling (Jiang and Liu 2008). In addition, PTEN is activated downstream of P2X7 (Mistafa, Ghalali et al. 2010; Miraglia, Hogberg et al. 2012; Ghalali, Wiklund et al. 2014). Consistent with activation of PTEN downstream of P2X7, inhibition of the phosphatase blocked geldanamycin toxicity (Fig. 7). In normal conditions, the over-activation of PI3K probably overwhelms the capacity of PTEN to decrease the levels of PIP3, keeping the pathway active and the motor neurons alive.

Trophic factor deprivation triggers Fas-dependent motor neuron apoptosis through the activation of two different pathways downstream of Fas receptor, a DAXX-dependent and a FADD-dependent pathway (Raoul, Henderson et al. 1999; Raoul, Estévez et al. 2002). While the DAXX-dependent pathway induces peroxynitrite production, the FADD-dependent component ultimately activates the cell death effector caspase 3. Our results show that depending on the concentration of inhibitor, inhibition of Hsp90 stimulated two different cell death mechanisms. In the presence of trophic factors, low concentrations of geldanamycin stimulated Fas-dependent apoptosis, while high concentrations also triggered Fas-independent motor neuron death (Fig. 2). The EC_{50} for the induction of motor neurons death by geldanamycin in the presence of trophic factors and Fas:Fc, a condition in which the Fas pathway is inhibited, was the same as the EC_{50} for the induction of death of trophic factor-deprived motor neurons. This observation provides further support to the conclusion that trophic factor deprivation and low

concentrations of geldanamycin stimulate the same death pathways in motor neurons. However, inhibition of Hsp90 did not require peroxynitrite production, as is the case for trophic factor deprivation (Estevez, Spear et al. 1998; Estevez, Sampson et al. 2000; Raoul, Estévez et al. 2002). Inhibitors of nitric oxide production and scavengers of superoxide and peroxynitrite had no effect on geldanamycin-induced motor neuron death (Fig. 3). We have recently identified Hsp90 as a target for peroxynitrite nitration. Nitrated Hsp90 triggers motor neuron apoptosis through the activation of the FADD component of the Fas pathway that is independent of peroxynitrite formation (Franco, Ye et al. 2013). Indeed, activation of the DAXX component of the pathway leads to peroxynitrite formation, nitration of Hsp90 and subsequent activation of the FADD-dependent pathway, inducing motor neuron apoptosis (Franco, Ye et al. 2013). The results showed here support the notion that both nitrated Hsp90 and inhibition of Hsp90 act downstream of peroxynitrite formation in the motor neuron death pathway. Both pathways are mediated by P2X7 and Fas activation. However, there are some differences between both mechanisms; while nitrated Hsp90-induced apoptosis is independent of gene expression and protein synthesis, geldanamycin-induced motor neuron death requires *de novo* synthesis of Fas ligand, as previously described for trophic factor deprivation (Raoul, Henderson et al. 1999; Barthelemy, Henderson et al. 2004). One very important difference between the two models is that nitrated Hsp90 stimulates cell death by a gain-of-function, while induction of motor neuron death by geldanamycin is due to a loss-of-function, which may explain the differences in the activation of the pathways. In spite of the differences, the requirement for P2X7 activation in both conditions suggests

that the inhibition of the purine receptor by Hsp90 is key for motor neuron survival. This inhibition seems to be easily perturbed by post-translational modifications or inhibition of the chaperone.

The nuclear factor FOXO3a regulates the expression of Fas ligand and several other pro-apoptotic proteins, including Bim (Barthelemy, Henderson et al. 2004; Behzad, Jamil et al. 2007). The activity of FOXO3a is negatively regulated by Akt activation, which results in retention of the factor in the cytoplasm (Brunet, Bonni et al. 1999; Tang, Nunez et al. 1999; Barthelemy, Henderson et al. 2004). Inactivation of the PI3K/Akt pathway by inhibition of Hsp90 prevented the phosphorylation of FOXO3a, allowing its activation, translocation to the nucleus (Fig. 4) and expression of Fas ligand. However, translocation of FOXO3a to the nucleus can also be neuroprotective in mixed spinal cord cultures. Overexpression of a constitutively active FOXO3a or treatment of motor neurons with psammaplysene, which reduces phospho-FOXO3a levels with no effect on AKT phosphorylation, effectively prevent motor neuron death induced by a number of noxious stimuli. However, direct inhibition of PI3K does not improve survival of motor neurons containing mutant SOD (Mojsilovic-Petrovic, Nedelsky et al. 2009). Our results are in agreement with a number of previous publications showing that inhibition of the PI3K pathway, which stimulates FOXO3a nuclear translocation, stimulates motor neuron death (Milligan, Prevette et al. 1995; Dolcet, Egea et al. 1999; Soler, Dolcet et al. 1999; Garces, Haase et al. 2000). In addition, the EC_{50} for cell death in dissociated cultures of spinal cord were 300 times higher than those necessary to trigger the death of 50% of the motor

neurons in pure cultures (Table 1), which can explain the absence of protective effect and the corroboration of the results using similar cultures (Barthelemy, Henderson et al. 2004).

In summary, the results reveal that Hsp90 inactivation of the purine P2X7 receptor is critical to prevent motor neuron apoptosis induced by activation of PTEN followed by inactivation of the Akt, dephosphorylation of FOXO3a and expression of Fas ligand.

CHAPTER 3: MUTANT SOD FACILITATES HSP90 NITRATION

Introduction

Mutations in the superoxide dismutase gene are associated with the development of Amyotrophic Lateral Sclerosis (ALS) (Deng, Hentati et al. 1993; Rosen, Siddique et al. 1993; Gurney, Pu et al. 1994; Wong, Pardo et al. 1995; Bruijn, Beal et al. 1997; Bruijn LI 1997; Martin, Price et al. 2000; Wong, Cai et al. 2002; Wang, Sharma et al. 2008; Wang, Deng et al. 2009). Under normal conditions, SOD converts superoxide to hydrogen peroxide and oxygen preventing oxidative stress (McCord and Fridovich 1969). However, mutant SOD induces neurodegeneration by an unknown and highly controversial toxic gain of function (Reaume, Elliott et al. 1996; Bruijn, Houseweart et al. 1998). Wild type SOD contains zinc and copper, which is responsible for enzyme stability and catalytic function. Mutant forms of SOD have reduced zinc affinity yet still retain copper (Lyons, Liu et al. 1996) suggesting a role for copper in the disease state. Immunohistochemistry of spinal cords from mutant SOD transgenic animals show intense nitrotyrosine immunoreactivity (Ferrante, Shinobu et al. 1997), a posttranslational modification associated with the production of reactive nitrogen species such as peroxynitrite. However transgenic animals expressing a SOD in which the residues that coordinate the copper were mutated (Quad SOD), still develop disease but with a slower progression (Subramaniam, Lyons et al. 2002). Extensive biochemical analysis of the

quad mutant SOD catalytic activity has yet to be performed. Consequently, the role of copper in the development of mutant SOD related toxicity is highly controversial.

Peroxynitrite is a powerful oxidant associated with the nitration of protein tyrosine residues. Peroxynitrite is formed by the diffusion limiting reaction between superoxide and nitric oxide (Beckman, Beckman et al. 1990; Padmaja and Huie 1993; Beckman and Koppenol 1996; Spear, Estévez et al. 1997; Nauser and Koppenol 2002). Nitration of Hsp90 by peroxynitrite has been shown to induce motor neuron cell death by a Fas dependent mechanism (Franco, Ye et al. 2013). Nitrated Hsp90 is present in a variety of neurological pathologies including spinal cord injury and ALS (Franco, Ye et al. 2013). However it remains unknown whether there is a link between SOD mutations and Hsp90 nitration in ALS.

More than 20 years after the original reports linking mutations on the gene of the SOD and ALS, the mechanism mutant SOD toxicity and the contribution of copper to the development of ALS remain unknown and highly controversial. Here we investigated the hypothesis that mutant SOD facilitates Hsp90 nitration, which in turn stimulates motor neuron death. Nitrated Hsp90 immunoreactivity was found in spinal cord motor neurons from patients and the G93A transgenic mouse model of ALS. Nitrated Hsp90 was present only in motor neurons at symptom onset and levels increase as disease progresses in the transgenic mouse model. Zinc deficient SOD and quad mutant SOD

bound Hsp90 and selectively facilitated the nitration of Hsp90. These results suggest that mutant SOD facilitate Hsp90 nitration within motor neurons.

Materials and Methods

Animal procedures: All procedures using laboratory animals were performed in accordance with the Guide for the Care and Use of Laboratory Animals of the National Institutes of Health. Male hemizygous NTac:SD-TgN(SOD1^{G93A})L26H rats (Taconic), were bred crossing with wild-type Sprague-Dawley female rats. Rats were housed with a 12-h light-dark cycle with ad libitum access to food and water. Symptomatic disease onset was determined by periodic clinical examination for abnormal gait, typically expressed as subtle limping or dragging of one hind limb. Rats were euthanized when reached disease end stage. All surgery was performed under 90% ketamine – 10% xylazine anesthesia, and suffering, discomfort or stress was minimized.

Histology: Animals were deeply anesthetized and transcardial perfusion was performed with 0.9% saline and 4% paraformaldehyde in 0.1 M PBS (pH 7.2–7.4) at a constant flow (1 mL/min). Fixed spinal cord was removed, post-fixed by immersion for 24 h, and then transverse sectioned serially (30–40 μm) on a vibrating microtome. Serial sections were collected in 100 mM PBS for immunohistochemistry. Free-floating sections were permeabilized for 30 min at room temperature with 0.3% Triton X-100 in PBS and passed through washing buffered solutions. Sections were blocked with 5% BSA:PBS

for 1 hour at room temperature, and incubated at 4 °C overnight with primary antibodies in 0.3% Triton X-100 and PBS [rabbit anti-Hsp90 (1:100, Santa Cruz Biotechnology), mouse-anti Hsp90 (1:200, Abcam) mouse anti-nitrated Hsp90 (1:200, Franco 2013), rabbit anti-GFAP (1:500, Sigma), rabbit anti-ChAT (1:300, Millipore), rabbit anti-humanSOD1 (1:500), and mouse anti-NO_2Tyr (1:200, (Franco, Ye et al. 2013))]. Immunoreactivity of nitrotyrosine was completely blocked by pre-incubation of the primary antibody with free nitrotyrosine (10 mM). After washing, sections were incubated in 1:1,000-diluted secondary antibodies conjugated to Alexa Fluor 488 and/or Alexa Fluor 633 (Invitrogen). Antibodies were detected by confocal microscopy using a confocal Olympus FV300 microscope.

Motor neuron isolation: Motor neurons were prepared as previously described (Henderson, Bloch-Gallego et al. 1995; Estevez, Spear et al. 1998; Raoul, Henderson et al. 1999). Motor neurons were plated on 96 well plates (1,000 cells per well), 4 well plates (2,000 cells per well), 8 well chamber (10,000 cells/well) or 4 well chamber (20,000 cells/well) coated with poly-DL-ornithine and laminin (Sigma). Motor neurons were maintained in motor neuron media [B27, heat inactivated horse serum, glutamine, glutamate, 3-mercaptoethanol (all from Gibco – Invitrogen, Carlsbad, CA) and trophic factors (1 ng/ml BDNF, 0.1 ng/ml GDNF, 10 ng/ml cardiotrophin-1) in neurobasal], and incubated in a 5% CO_2 humidified atmosphere at 37°C.

SOD delivery: SOD was delivered to motor neurons in suspension or after three days in culture. Recombinant protein was delivered as previously described [(Estévez, Crow et al. 1999), 1/265 dilution of chariot].

Immunoflourescence: Immunofluorescence was performed as previously described (Estevez, Spear et al. 1998). Cells were incubated with signal enhancer (Invitrogen) for 30 minutes before blocking. Primary antibodies for NO_2Hsp90, NO_2Tyr, and Hsp90 were incubated in blocking solution in a humidified chamber at 4°C overnight. Secondary AlexaFluor antibodies were incubated for 1 hour at room temperature, before staining with DAPI and mounting using ProLong Gold (Molecular Probes, Invitrogen, Eugene, OR).

Nitration assay: Recombinant protein (1 mg/mL in PBS) was added to brain homogenate (1 mg/ml in PBS) before the addition of peroxynitrite (0.5 mM) while vortexing. Samples were then diluted in lamelli buffer and processed as described previously (Franco, Ye et al. 2013). Western blots were performed using primary antibodies against NO_2Hsp90 (1/1,000, mouse), Hsp90 (1/1,000 rabbit), NO_2tyrosine (1/2,000, rabbit) and GAPDH (1/50,000, mouse). Secondary antibodies were obtained from Licor (1/25,000, anti-mouse and anti-rabbit).

Western blot analysis of tissue: For spinal cord protein extraction, spinal cords were completely dissected and embedded in lysis buffer [50 mM Hepes (pH 7.5), 50 mM

NaCl, 1% Triton X-100, and complete protease inhibitor cocktail (Sigma)] and sonicated six times for 3 s. Protein concentration was measured with Bicinchoninic Acid (BCA) kit (Sigma). Protein extracts were diluted in loading buffer (15% SDS, 0.3 M Tris (pH 6.8), 25% glycerol, 1.5 M β-mercaptoethanol, and 0.01% bromophenol blue). Protein samples (40 μg) were resolved on 12% SDS-polyacrylamide gel and transferred to PVDF membrane (Amersham). Membranes were blocked for 1 h in Tris-buffered saline (TBS), 0.1% Tween-20, and 5% non-fat dry milk, followed by overnight incubation with primary antibody [rabbit anti-Hsp90 (1:1,000, Santa Cruz), mouse anti-nitrated Hsp90 and mouse anti-β-actin (1:4,000, Sigma)] diluted in the same buffer. The membrane was incubated with peroxidase-conjugated secondary antibodies, Goat anti-mouse-HRP and Goat anti-rabbit-HRP (1:5000, Thermo) for 1 h and washed and developed using the ECL chemiluminescent detection system (Thermo). NO_2Hsp90 and Hsp90 (~90 kDa) bands were used to quantify the data. The intensities of all protein bands were normalized with the housekeeping gene, β-actin, using the ImageJ software.

Results

Nitrated Hsp90 was present in ALS patients. We have previously shown that nitration Hsp90 at residues 33 and 56 is necessary and sufficient to stimulate motor neuron apoptosis (Franco, Ye et al. 2013). Immunoreactivity for Hsp90 nitrated in tyrosine 56 (Ye, Quijano et al. 2007; Franco, Ye et al. 2013) was present in the spinal motor neurons from postmortem tissue of ALS patients, but could not be detected in the spinal cord of

age matched controls (Fig. 10). The immunoreactivity was prominent in motor neurons and could not de detected in other cell type. These results suggest that nitrated Hsp90 is present in spinal cord motor neurons of ALS patients before the cells die. These results suggest that nitrated Hsp90 can cause motor neuron degeneration in ALS.

Nitrated Hsp90 immunoreactivity was detected in motor neurons from symptom onset and increased with disease progression in the G93A mouse model of ALS. The time course of Hsp90 nitration in the spinal cord of G95A transgenic mouse model of ALS was determined to correlate the presence of nitrated Hsp90 with disease onset and progression. Nitrated Hsp90 was detected in ventral motor neurons during early symptomatic (90 days) and symptomatic stages (120 days) of the disease but not in presymtomatic (60 days), nontransgenic or mice transgenic for wild type SOD (Fig. 11A). The increase in glial fibrillary acidic protein (GFAP) immunoreactivity correlated with disease progression as previously reported (Schiffer, Cordera et al. 1996; Hall, Oostveen et al. 1998; Jaarsma, Teuling et al. 2008). Western blotting analysis of ventral spinal cord from transgenic mouse reveal significant increase in nitrated Hsp90 in symptomatic mice in comparison to nontransgenic animals, without changes in total Hsp90 (Fig. 11B). The results suggest that nitrated Hsp90 immunostaining represents an increase in the oxidative modification of Hsp90 rather than an increase in the amount of chaperone.

In addition, the GFAP and nitrated Hsp90 co-localize only in the late symptomatic phase, when significant motor neuron death already occurred (Fig. 11A). The presence of nitrated Hsp90 in astrocytes during the end stage of the disease could be due to nitration of astrocytic Hsp90 or to astrocyte phagocytosis of the motor neuron nitrated chaperone. To determine whether Hsp90 could be nitrated in the astrocyte, purified cortical and spinal astrocyte cultures were treated with peroxynitrite. Nitrated Hsp90 was not detected in cultured astrocytes 1 min or 24 hour after 5 min incubation with 1 mM peroxynitrite (Fig. 11C). Nitrated Hsp90 was in astrocyte homogenate incubated with peroxynitrite at the same concentration (Fig. 11C), suggesting that in astrocytes Hsp90 is protected from nitration. In aggregate, the results reveal that Hsp90 is nitrated in motor neurons during the symptomatic phase of ALS, which can explain symptom onset in ALS.

Mutant SOD increases protein nitration in vitro. Mutant SOD has reduced affinity to bind zinc, which is associated with increased protein nitration (Ischiropoulos, Zhu et al. 1992; Beckman, Carson et al. 1993; Crow, Strong et al. 1997). The role of zinc deficient SOD on nitration of Hsp90 was investigated by incubating nontransgenic spinal cord homogenate with peroxynitrite in the presence of zinc deficient SOD or wild type SOD. The nitrated homogenates were analyzed for nitrotyrosine and nitrated Hsp90. The addition of BSA was added to control for the effect of peroxynitrite alone on nitration of proteins. Zn deficient SOD produced an 8 fold increase in nitration as compared with the control or wild type SOD (Fig. 12A). These results corroborated previous reports

showing that zinc deficient SOD enhances peroxynitrite-mediated nitration (Crow, Strong et al. 1997). However, the relevance of copper in SOD toxicity is highly controversial. Transgenic animals for a SOD where the copper binding site has been deleted (Quad mutant) develop motor neuron disease (Wang, Slunt et al. 2003). This suggests that copper may not be required for mutant SOD toxicity. The presence of oxidative stress in this transgenic model animal was not tested. Incubation of spinal cord homogenates with peroxynitrite in the presence of quad mutant SOD increased protein nitration to levels comparable to Zn deficient SOD.

When the same samples were analyzed for nitrated Hsp90, both zinc and quad mutant SOD increased the levels of nitrated Hsp90 by 79 and 13 fold, which represents an increase of 10 and two fold respect to total nitration. In addition, wild type SOD had no effect on Hsp90 nitration (Fig. 12B). These results reveal that mutant SOD selectively enhances Hsp90 nitration by peroxynitrite.

Surface plasmon resonance was used to characterize the kinetics of the interactions of Hsp90 and SOD. Both Zn deficient, quad mutant SOD and APO C111S bound Hsp90, in contrast, no binding of fully metallated wild type SOD to Hsp90 was detected (Table 2). These findings suggest that Hsp90 bind partially and unmetallated SOD, which selectively increases the nitration of the chaperone.

Mutant SOD induce motor neuron cell death requires copper and peroxynitrite formation. The nitration of Hsp90 in the presence of quad mutant SOD suggests that this enzyme facilitate Hsp90 nitration because it has redox properties or due to a conformation change in the chaperone. To determine if quad mutant SOD induced motor neuron death in culture, recombinant protein was intracellularly delivered to motor neurons using the cell permeant agent, Chariot. Delivery of zinc deficient and quad mutant SOD stimulates motor neuron death (Fig. 13A). Similar treatment with copper deficient SOD did not affected motor neuron survival (Fig. 13A). The copper chelator, bathocuproine, prevented cell death induced by both zinc deficient and quad mutant SOD suggesting copper is required for the induction of cell death (Fig. 13B).

The delivery of both zinc deficient or quad mutant SOD to motor neurons resulted in increased immunoreactivity for nitrated Hsp90 (Fig. 13C). Protein nitration requires nitric oxide and peroxynitrite formation (Estevez, Spear et al. 1998; Estévez, Crow et al. 1999; Estevez, Sampson et al. 2000) therefore, the effect of nitric oxide synthase inhibitors on motor neuron survival was investigated. The nNOS inhibitor, L-NAME, prevented mutant SOD mediated motor neuron cell death indicating that production of nitric oxide is required for the induction of death (Fig. 13D). The superoxide dismutase mimetic, MnTBAP, and superoxide and peroxynitrite scavenger, FeTCCP, also prevented motor neuron death stimulated by Zn deficient and Q mutant SOD (Fig. 13D). These results suggest the zinc deficient and quad mutant SOD induce motor neuron death by a

similar copper dependent mechanism involving peroxynitrite formation and nitration of Hsp90.

The *in vitro* results suggest that the spinal cord of transgenic mice for the Q SOD should have nitrotyrosine. Indeed, the spinal cord of the mice transgenic for the quad mutant SOD showed intense immunoreactivity for nitrotyrosine (Fig. 14). However, the nitrotyrosine immunoreactivity was not as intense as that of aged matched transgenic animals for the G93A SOD mutation suggesting the rate of nitration is slower in the quad mutant animal (Fig. 14). These observations are in agreement with a slower development and progression of the disease in the quad mutant.

Discussion

Metal deficient SOD has reduced stability leading to protein unfolding (Rakhit, Crow et al. 2004; Rumfeldt, Lepock et al. 2009; Sahawneh, Ricart et al. 2010). The absence of nitrated Hsp90 in wild type samples suggests that SOD protein unfolding may increase Hsp90 susceptibility to nitration. Chaperone such as Hsp90 bind unfolded protein to prevent degradation and facilitate refolding.

The presence of nitrotyrosine in the spinal cord of ALS patients and animal models of the disease is well established (Abe, Pan et al. 1995; Beal, Ferrante et al. 1997; Ferrante, Shinobu et al. 1997; Duda, Giasson et al. 2000). However, the role that nitrotyrosine and oxidative stress play in the pathology of the disease is still highly controversial. Our

results reveal that the zinc deficient and quad mutant SOD induce motor neuron death by a similar copper dependent mechanism involving peroxynitrite formation and nitration of Hsp90 (Fig. 13A-D). We have previously shown that nitration of Hsp90 in tyrosine 33 or 56 is necessary and sufficient to make the chaperone toxic (Franco, Ye et al. 2013). We develop a monoclonal antibody against Hsp90 nitrated in tyrosine 56, which was fully characterized for specificity (Ye, Quijano et al. 2007; Franco, Ye et al. 2013). Using this antibody, we found that Hsp90 nitration occurs during the symptomatic phase of ALS and is found only within the motor neurons (Fig. 10). Nitrated Hsp90 immunoreactivity appears at symptom onset and coincides with motor neuron death.

Nitrated Hsp90 immunoreactivity was restricted to motor neurons in postmorterm spinal cord samples from ALS patients (Fig. 10) and in early stages of the disease in the spinal cord of the G93A mouse models of the disease (Fig. 11A and B). The inability of peroxynitrite to nitrate Hsp90 in cultured astrocytes (Fig. 11C) suggests that Hsp90 is protected from nitration in these cells. These results also suggest that nitrated Hsp90 in astrocytes at end stages of the disease is likely due to the removal of motor neuron debris by astrocytes rather than nitration of the astrocyte Hsp90. The specific formation of nitrated Hsp90 in motor neurons may explains how glial cell specific knockdown of mutant SOD has no effect on disease onset and why neuron specific expression of mutant SOD is enough to produce disease (Boillee, Yamanaka et al. 2006; Jaarsma, Teuling et al. 2008; Yamanaka, Chun et al. 2008).

Peroxynitrite nitration can by catalyzed by SOD and the catalysis is enhanced in zinc deficient SOD (Ischiropoulos, Zhu et al. 1992; Crow, Sampson et al. 1997; Adams, Franco et al. 2015). Although original reports on the Q mutant showed that the enzyme has no superoxide dismutase activity, the metal content of the enzyme or other redox properties were not investigated (Wang, Slunt et al. 2003). Our result show enhanced tyrosine nitration by peroxynitrite in the presence of quad mutant, suggesting that the protein possess redox activity. In fact the increase in nitration was similar to the nitration catalyzed by Zn-deficient SOD (Fig. 12A). Furthermore, motor neuron death stimulated by Q mutant, and Zn-deficient SOD were prevented by inhibition of nitric oxide production, and scavenging of superoxide and peroxynitrite (Fig. 13D). This provides further support for a redox mechanism mediated by Q SOD in the pathogenesis of the transgenic mouse. In addition, quad mutant SOD induced motor neuron death in culture was preceded by the nitration of Hsp90. In fact, both Zn-deficient and Q mutant selectively facilitated the nitration of Hsp90 (Fig. 13C). The enhanced nitration could be caused by increase catalysis, but it can also be caused by changing the conformation of Hsp90 to become more favorable to nitration. Metal deficient SOD has reduced stability leading to protein unfolding (Rakhit, Crow et al. 2004; Rumfeldt, Lepock et al. 2009; Sahawneh, Ricart et al. 2010). The absence of nitrated Hsp90 in wild type samples suggests that SOD protein unfolding may increase Hsp90 susceptibility to nitration. However, wild type SOD did not bind Hsp90 (table 2), suggesting that the interaction with Hsp90 may be due to the unfolding of SOD, or a specific SOD conformation provided by partially metillated proteins. ALS linked mutations in SOD have been

shown to have a reduced zinc affinity (Lyons, Liu et al. 1996; Crow, Sampson et al. 1997) that leads to destabilization of the dimer and protein unfolding (Rumfeldt, Lepock et al. 2009; Sahawneh, Ricart et al. 2010). As a consequence, there is increased aggregation of the mutant SOD monomers (Rakhit, Crow et al. 2004; Rumfeldt, Stathopulos et al. 2006; Rumfeldt, Lepock et al. 2009). These mutants favor a zinc deficient monomer, where copper remains bound (Rumfeldt, Lepock et al. 2009; Sahawneh, Ricart et al. 2010). Mutant SOD unfolding leads to the interaction with chaperones such as Hsp70 (Shinder 2001). Interestingly, the degree of instability of the APO state of SOD correlates to length of survival (Sato 2005) and this relationship may be due Hsp90 binding to mutant SOD and subsequent nitration. The direct interactions of mutant SOD to heat shock chaperones such as Hsp70 and Hsp90 may facilitate nitration. However, only Hsp90 is responsible for induction of motor neuron death (Franco, Ye et al. 2013). Nitrated Hsp90 stimulates motor neuron death by a P2X7 receptor/Fas dependent pathway that is consistent with a downstream effector of mutant SOD stimulated motor neuron death (Raoul, Estévez et al. 2002).

Our results demonstrate that quad mutant SOD toxicity is dependent on copper (Fig. 13B). These results are contrary to previous findings where transgenic mutant SOD animals crossbred with animals containing a genetic deletion of the copper chaperone for SOD (CCS) still developed motor neuron disease (Subramaniam, Lyons et al. 2002). These animals had a 90% reduction of copper incorporation into mutant SOD, however the remaining copper containing SOD may be enough for the animal to develop the

disease (Beckman, Estévez et al. 2001). The dependency of the quad mutant SOD to bind copper suggests the presence of an alternative binding site. Since this site is a secondary binding site it is possible that the copper binding changes the enzyme's confirmation reducing its ability to facilitate protein nitration leading to slower disease progression. Many of the argument against the role of redox properties of SOD playing a role in the pathogenesis of ALS come from genetic studies in which the biochemistry of the enzyme was not investigated at all or poorly characterized. The presence of markers of oxidative damage such as nitrotyrosine in all animal models of the disease and post mortem samples of ALS patients coupled with a number of studies showing how these markers stimulate motor neuron death, provide the best rounded hypothesis for ALS pathogenesis. The presence of nitrated Hsp90 in motor neurons of both animal models and human patients provide the first complete pathway explaining ALS pathology.

Our findings demonstrate that mutant SOD facilitates Hsp90 nitration in motor neurons in a copper and peroxynitrite dependent mechanism. Hsp90 nitration occurs at disease onset and increases during disease progression in a G93A transgenic animal. In contrast, astrocytes are not nitrated during disease onset nor do they become nitrated in vivo. These results suggest that mutant SOD induce cell autonomous neuronal cell death through nitrated Hsp90.

CHAPTER 4: CHRONIC INHIBITORY EFFECT OF RILUZOLE ON TROPHIC FACTOR PRODUCTION[1]

Introduction

Amyotrophic lateral sclerosis (ALS) is a devastating and incurable neurological disease, characterized by the degeneration of pyramidal neurons in the motor cortex and motor neurons in the brain stem and spinal cord. ALS patients live without medical intervention an average of one to five years following diagnosis. Riluzole is the only drug that shows a small but consistent protective effect both in patients and transgenic mice models of ALS (Bensimon, Lacomblez et al. 1994; Gurney, Cutting et al. 1996; Lacomblez, Bensimon et al. 1996; Lacomblez, Bensimon et al. 1996; Gurney, Fleck et al. 1998; Orrell 2010; Miller, Mitchell et al. 2012). Riluzole has been shown to block sodium channels, activate G-proteins and reduce glutamate toxicity (Doble 1997; Meininger, Lacomblez et al. 2000; Cheah, Vucic et al. 2010; Bellingham 2011). However, the primary mechanism by which riluzole exerts its protective effects in ALS remains unknown.

Astrocytes and other glial cells produce trophic factors that support motor neuron

---

[1] Dennys, C. N., J. Armstrong, et al. (2015). "Chronic inhibitory effect of riluzole on trophic factor production." Exp Neurol.271:301-307.

survival (Schnaar and Schaffner 1981; Eagleson, Raju et al. 1985; Eagleson and Bennett 1986; Ang, Bhaumick et al. 1993; Arce, Pollock et al. 1998). Riluzole enhances the astrocytic production of these factors in cell culture (Peluffo, Estévez et al. 1997). The incubation of cortical astrocytes with riluzole stimulates the production of brain derived neurotrophic factor (BDNF), glia derived neurotrophic factor (GDNF) and nerve growth factor (NGF) (Mizuta, Ohta et al. 2001). Schwann cells also produce trophic factors that promote axon regeneration following exercise and nerve injury (Wilhelm, Xu et al. 2012; Xu, Rosen et al. 2013). Cardiotrophin-1 (CT-1) is a potent motor neuron trophic factor that prevents motor neuron death after axotomy and delays death in animal models of ALS produced by muscle (Pennica, Arce et al. 1996; Bordet, Lesbordes et al. 2001).

Initial studies on the effect of riluzole lead us and others to postulate that riluzole may exert at least in part its protective effects on motor neurons indirectly, by promoting trophic factor production by astrocytes and other glial cells (Peluffo, Estévez et al. 1997; Mizuta, Ohta et al. 2001). Here we investigated the effects of short and long time incubation with riluzole on trophic factor production by Schwann cells and astrocytes. Both cell types play an important role in cellular maintenance of motor neurons. We investigated also concentrations of trophic factors produced in brain, spinal cord, and sciatic nerve of C57BL/6J mice at different time points after continuous or discontinuous riluzole administration and correlated the *in vivo* results to specific glial cell responses. Our findings provide new insights on the potential mechanism of action of riluzole as a therapeutic treatment for ALS and possibly spinal cord injury.

Materials and Methods

Astrocyte cell culture: Spinal cords from one to three days old Sprague Dawley rats were used to prepare astrocytes as described previously (Saneto and Vellis 1987; Peluffo, Estévez et al. 1997). Once confluent (approximately 5-8 days), cells were shaken at 300 RPM for 2 days then treated with 10 μM arabinose C. Following a couple days recovery, cells were split and seeded on a 60mm dish at a density of one million cells or half a million for a 35mm dish. Cells were maintained in culture for no more than 22 days.

Motor neuron cell culture: Rat embryo motor neurons were purified using 6% OPTI prep and further purified using immunoaffinity. Cells were cultured in neurobasal medium containing glutamine, glutamate, β-mercaptoethanol, and B27 supplement (Gibco-Invitrogen) as previously described (Estevez, Spear et al. 1998; Pettmann and Henderson 1998; Raoul, Henderson et al. 1999) in the presence or absence of brain-derived neurotrophic factor (BDNF, 1 ng/mL), glial-derived neurotrophic factor (GDNF, 0.1 ng/mL), and cardiotrophin 1 (CT-1, 10 ng/mL). Motor neuron survival was determined by counting by hand in four well plates (Nunc) or by calcein staining (Molecular Probes, Invitrogen) according to manufacturer's instruction. Extracellular calcein was quenched with 100 μg/mL hemoglobin and the images were captured using the RUNNER (Trophos, Marseilles, France). Data was analyzed using Tina software (Trophos).

Schwann Cell culture: Primary Schwann cells were isolated from the sciatic nerves of newborn Sprague Dawley rats with modifications as previously described (Brockes, Fields et al. 1979; Thaxton, Bott et al. 2011). 250,000 cells (35 mm dish) or 500,000 cells (60 mm dish) were grown in D10M (10% FBS, 20 µg/ml pituitary extracts and 2µM forskolin in DMEM) on poly-L-lysine coated plates (200 µg/mL) until confluency. Media was changed three days before the experiment was started. Experiments were conducted on Schwann cells that were passaged no more than four times.

Conditioned Media: Astrocytes or Schwann cells were treated with 1 µM riluzole for indicated time period. For chronic treatments, media was changed with fresh riluzole every 2-3 days. Media was removed and cells were washed with DPBS prior to addition of conditioning media (L15 supplemented with sodium bicarbonate (22 mM), conalbumin (0.1 mg/ml), putrescine (0.1 mM), insulin (5 µg/ml), and sodium selenite (31 nM). Astrocytes or Schwann cells conditioned this media for 24 hours prior to collection. Conditioned media was further diluted in motor neuron media prior to plating motor neurons. Motor neurons were cultured in the presence of conditioned media for three days then counted.

PCR Analysis: RNA was extracted from Schwann cells plated on a 35 mm dish using Trizol. 1 µg RNA was used to synthesize cDNA using Superscript III (Invitrogen) according to manufacturer's instruction. 2 µl of cDNA product was used as template for

qPCR analysis. CT-1, BDNF, and GDNF levels were measured using Taq Man probes and master mix according to manufacturer's instruction.

Animal Studies: Male C57BL/6J mice were given riluzole treated water (100 μg/ml) for given time points. Water was replaced with freshly prepared riluzole every 2-3 days. Brain, spinal cord, and sciatic nerve were removed for subsequent analysis. Untreated mice were sacrificed for control.

ELISA: Brain, spinal cord, and sciatic nerve were homogenized in PBS containing PMSF, and protease inhibitor cocktail. Samples were diluted to a concentration of 175 μg/mL and analyzed using ELISA [CT-1 (R & D Systems), BDNF and GDNF (Abnova)]. ELISA was performed according to manufacturer's instructions.

Results

Riluzole treatment stimulates glial cells to produce CT-1. Riluzole stimulates trophic factor production by astrocytes (Peluffo, Estévez et al. 1997; Mizuta, Ohta et al. 2001). Incubation of motor neurons with media that was previously conditioned by astrocytes in the presence of 1-10 μM riluzole significantly increases motor neuron survival when compared to cells cultured in conditioned media from untreated astrocytes (Peluffo, Estévez et al. 1997). Since the trophic factors BDNF, GDNF and CT-1 are critical to motor neuron survival, we investigated the effect of riluzole on production of these trophic factors by astrocytes using conditions previously described (Peluffo, Estévez et

al. 1997). There was a small, but statistically significant change in CT-1 mRNA levels with no change in mRNA levels of BDNF, and GDNF of riluzole treated astrocytes when compared to untreated controls (Fig. 15A). Since mRNA levels do not reflect protein levels, neutralizing antibodies to BDNF, GDNF and CT-1 were used to determine the effect of each trophic factor present in conditioned media on motor neuron survival. Motor neurons were cultured in the absence of trophic factors and survival was assessed after 24 h in culture. Incubation of motor neurons with media that was previously conditioned by astrocytes for 24 h partially protected motor neurons from trophic factor deprivation-induced cell death (Fig. 15B). This protection was significantly increased by conditioned media from astrocytes that were incubated in the presence of riluzole for 24 h prior to media conditioning (Fig. 15B). Antibodies against CT-1 had no effect on motor neuron survival in the presence of conditioned media from untreated astrocytes, but blocked the additional protection afforded by the media from riluzole-treated astrocytes (Fig. 15A), suggesting that CT-1 production is stimulated by riluzole. As expected, addition of antibodies against GDNF or BDNF also reversed the protection provided by riluzole treated astrocyte conditioned media (Fig. 15B) since these factors are basally secreted by astrocytes (Schaar, Sieber et al. 1993; Dougherty, Dreyfus et al. 2000; Jean, Lercher et al. 2008; Fulmer, VonDran et al. 2014). These results imply that in addition to stimulate the production of BDNF and GDNF by cortical astrocytes (Mizuta, Ohta et al. 2001), riluzole also induces the synthesis and release of CT-1 by spinal astrocytes.

Schwann cells provide trophic factor support for motor neurons under stress conditions (Wilhelm, Xu et al. 2012; Xu, Rosen et al. 2013). Therefore we investigated if riluzole could also stimulate trophic factor production in these cells at the same concentrations of drug used for astrocytes. Initial experiments were conducted to determine the dilution of riluzole-treated and untreated Schwann cell conditioned media that would provide discernable differences in trophic factor support. Due to a higher level of trophic support in Schwann cell conditioned media, a 1:25 dilution was selected to perform subsequent experiments compare to the 1:10 dilution applied to conditioned media from astrocytes (Sup. Fig. 1A). Incubation of Schwann cells with riluzole for 24 h prior to conditioning the media significantly increased the protection provided to motor neurons in comparison to media from untreated cells (Fig. 15C). Neutralizing antibodies against CT-1 completely abolished the protection afforded by conditioned media from riluzole-treated Schwann cells (Fig. 15C). In the same conditions, neutralizing antibodies against BDNF and GDNF had no effect on motor neuron survival (Sup. Fig. 1B). In contrast, neutralizing antibodies against GDNF but not BDNF, reduced motor neuron survival in untreated conditioned media (Sup. Fig. 1B). In agreement with these observations, the levels of CT-1 messenger RNA were significantly increased after 24 h incubation with riluzole, while no changes were detected for GDNF and BDNF messenger RNAs (Fig. 15D). These results reveal that Schwann cells in culture produce CT-1 and that the production and release of CT-1 is enhanced by riluzole. Incubation of astrocytes and Schwann cells with riluzole had no effect on cellular morphology or number (Sup. Fig. 1A and B). Together, these results show that riluzole treatment increases trophic factor

deprived-motor neuron survival by inducing release of CT-1 by both astrocytes and Schwann cells.

Chronic riluzole treatment decreases trophic factor production by glial cells: Since incubation of astrocytes and Schwann cells with riluzole for 24 h showed an increase in trophic factor production, we investigated whether longer incubation periods would results on higher and more stable production of trophic factors by glial cells. Surprisingly, incubation of astrocytes with riluzole for up to 6 days prior to media conditioning resulted in a significant reduction of the protection provided to motor neurons when compared with conditioned media from astrocyte cultures incubated with riluzole for 24 h (Fig. 16A). To determine if the loss of the astrocytes response to riluzole was the result of the chronic incubation with riluzole or astrocyte senescence, parallel astrocyte cultures were maintained in the same conditions, but in the absence of riluzole. These cultures were then treated with riluzole for 24 h prior to conditioning the media (5U1R, as described in Fig. 16A). Conditioned media from these cultures had a motor neuron trophic activity comparable to that of conditioned media from acute riluzole treated astrocyte (1R, Fig. 16A) and increases motor neuron survival above six days untreated astrocytes. These results reveal that conditioned media derived from astrocytes after chronic incubation with riluzole had reduced trophic support.

When the same experimental design was applied to Schwann cells, after 5 days in culture followed by 24 h incubation with riluzole the cells failed to respond to the drug (5U1R).

However, conditioned media from acute treatment (1R, Sup. Fig. 1C) was indeed protective. Quantitative RT-PCR showed a significant reduction in CT-1 levels after 3 days of continuous incubation with riluzole while after 6 days in culture the cells became senescent. Therefore, conditioned media from Schwann cells incubated with riluzole for 3 days was considered a long-term treatment with the drug. In agreement, this conditioned media showed reduced motor neuron trophic factor support (Fig. 16B), while the control riluzole treatment, 2 days in culture followed by 24 h incubation with the drug (2U1R, Fig. 16B) maintained motor neuron survival to levels comparable to acute riluzole incubation (1R, Fig. 16B) and increased motor neuron survival above 3 day untreated cells. Long-term incubation of astrocytes and Schwann cell produced no change on the morphology or proliferation of the cells (Sup. Fig. 2A-C). These observations revealed that the long-term effects of riluzole were not due to loss of cell responsiveness to the drug. In addition, the expression of CT-1 and BDNF messenger RNA in Schwann cells was decreased after long-term incubation with riluzole compared with one-day incubation, with the expression of BDNF mRNA lower than untreated control (Fig. 16D). In astrocytes, long-term incubation with riluzole decreased expression of CT-1 compared with cultures treated for one day with the drug. Interestingly, BDNF and GDNF, but not CT-1 mRNA expression was below untreated control in astrocytes after 6 days riluzole incubation (Fig. 16C). These results suggest that the effect of riluzole on the regulation of trophic factors mRNA expression is trophic factor and cell type specific. Together these findings suggest that chronic exposure to

riluzole significantly reduces trophic factor production by glial cells, abolishing the protective effect observed on trophic factor deprived-motor neurons.

Acute and chronic riluzole treatment has opposite effects on trophic factor production in vivo: The effects of riluzole on trophic factor production were investigated in spinal cord, whole brain and sciatic nerve of C57BL/6J male mice after treatment with riluzole in the drinking water for various time periods. In the spinal cord, riluzole significantly increased CT-1 levels after 15 days of continuous treatment. However, the increase was only transitory since CT-1 production was reduced to basal levels after 30 days of treatment (Fig 17A). In contrast, riluzole did not stimulate BDNF production at any time, but induced a significant decrease of BDNF levels after 30 days of treatment (Fig. 17A). GDNF production was significantly increased after 3 days of riluzole treatment and returned to basal levels after 6 days of continuous administration of the drug. Surprisingly, GDNF production decreased below control levels after 15 and 30 days of continuous treatment (Fig. 17A). These observations cannot be attributed to differences in drug intake since there were no changes in the water consumption by the mice throughout the study (6.5-7.5 ml/animal/day, independently of the treatment). Thus, these findings are consistent with the repressive effects on BDNF, GDNF, and CT-1 production observed in cell culture after long-term incubation of astrocytes with riluzole.

In the sciatic nerve, treatment with riluzole increased CT-1 levels at 3 and 15 days. However, CT-1 levels were significantly decreased below control levels after 30 days of

continuous treatment with the drug (Fig. 17B). Riluzole did not increase GDNF or BDNF concentration in the sciatic nerve but BDNF level was significantly decreased after 30 days of riluzole treatment. These findings are consistent with the repressive effects on BDNF and CT-1 production observed in Schwann cells following chronic treatment of riluzole in culture.

In the brain, CT-1 levels increased only at 6 days, returning to basal levels at 15 and 30 days of continuous riluzole administration. Riluzole did not stimulate significant changes in GDNF concentration at any time, but increased BDNF concentrations in the brain after 6 and 15 days treatment. After 30 days of continuous riluzole administration, the BDNF concentration was reduced below control levels (Fig. 17C). These results reveal that acute riluzole treatment activated the production of distinct combinations of CT-1, GDNF and BDNF in spinal cord, sciatic nerve and brain at different times. However, the chronic treatment with riluzole led to a significant reduction of trophic factor production, in some cases below the control levels.

Discontinuous riluzole treatment increases long-term CT-1 production in spinal cord: The opposite effects of the chronic and acute administration of riluzole in the animals lead us to investigate 1) whether the acute stimulatory effect could be maintained by discontinuous administration of the drug, and 2) whether the chronic inhibitory effect could be reversed. As shown in Fig. 3, trophic factor levels were elevated between 3 and 15 days then reduced by 15 or 30 days depending on the trophic factor and the tissue.

Based on these results, animals were continuously administered riluzole for 15 and 30 days then riluzole was removed for 15 days. The treatment was then reinitiated for additional 6 or 15 days to avoid the chronic inhibitory effect (Fig. 18A). Trophic factor levels were studied in spinal cord from treated animals. After the second period of riluzole administration, CT-1 concentration was significantly increased as compared to the untreated control independently of whether the drug was given for 15 or 30 days during the initial period (Fig. 18B). In the case of GDNF, continuous treatment with riluzole for 15 or 30 days decreased the trophic factors levels. This decrease could not be reverted by discontinuing the treatment for 15 days and treating with the drug for additional 6 or 15 days (Fig. 18C). Moreover, treatment of animals for 30 days with 15 days resting period and 15 additional days with riluzole showed significantly more reduction in GDNF concentrations than animal continuously treated with riluzole for 30 days (Fig. 18C). The concentration of BDNF was not increase respect to the control in any condition (Fig. 18D). Similar to GDNF, BDNF levels in the spinal cord were significantly reduced after treatment of animals with riluzole for 30 days with a 15 days rest period than after 30 days of continuous administration (Fig. 18D). In combination, these observations suggest a complex regulation of the expression of trophic factors by riluzole.

Discussion

Riluzole is the only FDA approved drug for the treatment of ALS. However, the primary mechanism by which riluzole offers protection remains unknown. In both spinal cord organotypic and enriched motor neuron cultures riluzole protects motor neurons from glutamate receptor hyperstimulation-induced death (Estevez, Stutzmann et al. 1995; Rothstein and Kuncl 1995). These original observations are supported by new evidence of the anti-excitotoxic effect of the drug in ALS patients (Bellingham 2011; Cifra, Mazzone et al. 2013; Foerster, Pomper et al. 2013; Vucic, Lin et al. 2013). However, these same reports conclude that the effects of riluzole on glutamate metabolism are not sufficient to explain its protective effects in ALS. After the failure of the gabapentin clinical trial, riluzole was postulated to act on pathways other than the glutamatergic transmission (Meininger, Lacomblez et al. 2000). Riluzole stimulates trophic factor production by astrocytes (Peluffo, Estévez et al. 1997; Mizuta, Ohta et al. 2001). However, the effect of riluzole on trophic factor production in other cell types was not investigated. Motor neuron survival is supported by trophic factors released by Schwann cells during development (Henderson, Phillips et al. 1994) and nerve regeneration (Xu, Rosen et al. 2013) but whether Schwann cells supported motor neuron survival in adult normal conditions remained unknown. Here, we show for the first time that Schwann cells produce CT-1 in these conditions. Although Schwann cell production of BDNF and GDNF contribute also to motor neurons survival in culture, CT-1 was the only factor induced in Schwann cells following riluzole treatment. Results using conditioned media

from riluzole-treated Schwann cells support CT-1 as the major trophic factor induced by riluzole, since neutralizing antibodies against CT-1 reduced motor neuron survival to levels comparable to those of untreated conditioned media. Similar findings were obtained with conditioned media from riluzole-treated astrocytes (Fig. 15). Previous reports shows that riluzole induces secretion of NGF, BDNF, and GDNF by cultured cortical astrocytes (Mizuta, Ohta et al. 2001). In contrast with these observations, acute incubation of spinal cord astrocytes with riluzole led to a significant increase in secretion of CT-1 but not BDNF or GDNF (Fig. 17). However, in the brain of mice after acute treatment with riluzole, CT-1 and BDNF production was induced, without affecting GDNF levels. These discrepancies between the cell culture and *in vivo* tissue effects may be due to direct or indirect effects of riluzole on other cell types. The difference in trophic factor production in the examined tissue suggests that responses to riluzole depend on the cell specific population within the corresponding tissue. Surprisingly, long-term riluzole treatment of Schwann cells and astrocytes with riluzole resulted in a significant reduction of trophic activity (Fig. 16), suggesting a biphasic stimulatory-inhibitory effect of riluzole on the production of trophic factors.

The regulation of the concentration of different trophic factors by oral administration of riluzole to mice was tissue and time dependent (Fig. 17). While some trophic factors were initially increased over basal concentrations, all trophic factors concentrations dropped to basal levels and in some cases below basal levels after longer treatment with riluzole. In agreement with the cell culture results, CT-1 was the only trophic factor

consistently induced after acute treatment of mice with riluzole in spinal cord, sciatic nerve and brain (Fig. 17). BDNF and GDNF concentrations were initially increased in some tissues, but not others. However, chronic treatment reversed to basal or below control levels for all three trophic factors (Fig. 17). The half-life of riluzole *in vivo* is measured in hours. In the nervous system, riluzole is removed at the level of the blood-brain barrier by the P-glycoprotein (Milane, Fernandez et al. 2007; Milane, Vautier et al. 2009; Milane, Fernandez et al. 2010; Dulin, Moore et al. 2013). In patients and models of ALS both drug efflux transporters, P-glycoprotein and breast cancer-resistant protein (BCRP) are increased. Gene deletion of P-glycoprotein or pharmacological inhibition of these transporters provides a small protective effect when riluzole is administer at disease onset in the G93A mouse model of ALS (Jablonski, Markandaiah et al. 2014). This enhanced protection by riluzole is consistent with our observation of acute effects increasing trophic factor production. However, decreased concentrations of riluzole in the nervous system could explain the return of the trophic factor concentrations to basal control levels, but not below those levels, suggesting there is a secondary inhibitory effect mediated by riluzole itself or by a metabolic product of riluzole that remains to be identified.

Riluzole is undergoing clinical trials for the treatment of spinal cord injury and repair. In order to maximize its therapeutic effects riluzole must be administered within hours of injury (Nogradi, Szabo et al. 2007). Thus, riluzole may be effective for treatment in spinal cord injury and repair in these conditions because trophic factor production by

astrocytes is induced locally at the critical time to prevent neuronal death and to facilitate axonal regeneration and growth (Li, Oppenheim et al. 1994; Bergerot, Shortland et al. 2004). These findings suggest that induction of the specific trophic factors in the right cells could be critical to achieve the desired beneficial therapeutic effect in spinal trauma. Most animal studies were conducted using continuous administration of riluzole for 2-3 weeks (Nogradi and Vrbova 2001; Bergerot, Shortland et al. 2004; Nogradi, Szabo et al. 2007; Dennys, Franco et al. 2014), which could result in a decreased of the potential beneficial effects. However, it is also possible that the long-term treatment with riluzole induces an initial increase in trophic support, which helps axon regenerate through the affected area. Conversely, the chronic effect of riluzole could also be beneficial in this context, by decreasing the local production of trophic factors, which allows axons to leave the affected area to interact with the right targets.

Trophic factors have shown to be protective in animal models of ALS. However, the translation to clinical trials resulted in failure. Most trophic factors investigated in clinical trials for ALS have been unsuccessful at extending patient survival (Group 1996) These trials used invasive delivery methods to ensure the trophic factor of interest would cross the blood brain barrier (Kastin, Akerstrom et al. 2003; Dennys, Franco et al. 2014). In summary, there are multiple factors that can explain trophic factors failure in clinical trails, including secondary effects due to systemic administration (Gould and Oppenheim 2011). The success of riluzole may be due to the stimulation of the local production of trophic factor by motor neuron associated cells. However, independently of the

mechanism of riluzole action, here we show that riluzole regulates protein expression and it has opposite effects on the production of trophic factors. Early stimulation of trophic factor production is followed by a decrease, in some cases below basal levels, which strongly suggest the second phase is not a consequence of loss of activity or habituation but inhibition of trophic factor production. Modifying the dosing regimen of riluzole may maximize the protective effects of the glial-derived trophic activity necessary to improve treatment of patients with ALS. We showed that discontinuous administration of riluzole maintained elevated CT-1 levels in the spinal cord *in vivo* (Fig. 18). However, these same protocols of discontinuous riluzole treatment did not prevent down regulation of BDNF or GDNF. In the case of GDNF, after 15 days treatment with riluzole with a 15 days rest period, the concentrations of the trophic factor were not affected by further administration of the drug. In contrast, when the initial period of riluzole administration was 30 days, the additional treatment with riluzole further decreased the concentrations of GDNF, suggesting that some of the chronic effects of riluzole could be irreversible or take a very long time to reverse.

Riluzole readily crosses the blood brain barrier and in addition to stimulate trophic factor production in glial cells, it has direct effects on motor neurons and maybe other yet unknown protein synthesis-dependent effects. Optimizing the administration protocols could avoid potential negative chronic effects such as the decrease of trophic factors levels described here. In addition, it is possible that the modest effects of riluzole in ALS are due to a combination of acute protective effects and chronic negative effects.

However, this biphasic effect may be actually beneficial in other conditions such as spinal cord injury. The initial protective effect of riluzole could help neuronal survival and axon growth through the damaged area. The secondary inhibition of trophic factor production might allow axons to leave the damaged area and reach their targets, thus reversing the damage. Optimizing the administration conditions for riluzole would depend on the pathology to be treated and the development of good peripheral markers of riluzole action in the central nervous system to adjust dosage according to the response of the patient.

CHAPTER 5: GENERAL DISCUSSION

The inability of neurons to replicate makes their loss particularly devastating to the nervous system as new cells cannot be generated to replaced lost ones. Therefore the nervous system has unique mechanisms to maintain motor neuron survival. The inability of motor neurons to initiate a stress response appears counter intuitive in this context. Consequently, the role of heat shock chaperones has been extensively studied as a potential therapeutic target in neurodegeneration (Bruening, Roy et al. 1999; Batulan, Shinder et al. 2003; Robinson, Tidwell et al. 2005; Batulan, Taylor et al. 2006; Gifondorwa, Robinson et al. 2007; Robinson, Gifondorwa et al. 2010). We have shown that Hsp90 plays a critical role in motor neuron survival due to its repressive effects on the purine receptor P2X7 (P2X7R). Activation of P2X7R leads to inhibition of the PI3K/AKT pathway and Fas mediated apoptosis. The atypical stress response may be due to the repressive effects of Hsp90 on P2X7R. Removal of Hsp90 from this repressive complex under conditions of stress, would lead to motor neuron death.

Significant motor neuron death is found at disease onset and increases as disease progresses in transgenic mutant SOD animals models (Bruijn, Becher et al. 1997) (Vinsant, Mansfield et al. 2013). However the mechanism behind mutant SOD toxicity remains to be identified. We show that mutant SOD facilitates nitration of Hsp90. Nitrated Hsp90 has been shown to activate P2X7 leading to cell surface expression of FasL and subsequent activation of FasR without transcriptional activation of Fas (Franco,

Ye et al. 2013). This suggests that mutant SOD facilitated Hsp90 nitration may be inducing motor neuron cell death by the same mechanism. These findings explain why P2X7R inhibitors are protective in animal models for ALS (Apolloni, Amadio et al. 2014). However motor neuron cell death induced following inhibition of Hsp90 involves a slightly different mechanism. Inhibition of Hsp90 leads to inhibition of the PI3K/AKT pathway and subsequently induces FasL expression. This difference provides evidence for a toxic gain of function for nitrated Hsp90.

ALS pathology has been attributed to both a cell autonomous and non-cell autonomous processes. Transgenic animals containing genetic deletion of neuronal mutant SOD still develop the disease (Boillee, Yamanaka et al. 2006). This suggests a glial contribution to disease pathology. Conditioned media and co-culture experiments indicate that astrocytes secrete a soluble factor that induces motor neuron death (Pehar, Cassina et al. 2004; Nagai, Re et al. 2007; Aebischer, Cassina et al. 2010; Diaz-Amarilla, Olivera-Bravo et al. 2011; Basso, Pozzi et al. 2013; Re, Le Verche et al. 2014). Therapeutic targeting of these cells to secrete trophic factors is a potential therapeutic treatment for ALS. We show that acute treatment with riluzole induces trophic factor production in astrocytes and Schwann cells. Therefore, treatment with riluzole could prevent the toxic effects observed of glial cells in ALS. However, long-term treatment with riluzole reduces trophic factor levels to equal or below untreated cell types. Therefore the current dosing regimen of twice a day for ALS patients could be detrimental in the long-term. Discontinuous riluzole treatment in animals can maintain elevated levels for trophic

factors and prevent trophic factor reduction in a factor specific manor. This suggests that optimizing a discontinuous riluzole treatment in ALS patients may extend lifespan in ALS patients.

Nitrated Hsp90 has been implicated in other disease states including spinal cord injury (Franco, Ye et al. 2013). The ability of a normal cell to induce nitration of Hsp90 suggests a signaling capability of this modification. Therefore it could be possible for Hsp90 to be nitrated in circumstances that does not involve mutant SOD. One such instance is in cases of sporatic ALS, where the cause of motor neuron disease is unrelated to genetics. Certain stress related triggers, such as metal depleted wild type SOD (Rotunno and Bosco 2013), may induce Hsp90 nitration leading to motor neuron death and ALS pathology. Therefore nitration of Hsp90 may explain disease pathology in ALS cases with unknown cause.

In summary, we have identified Hsp90 and P2X7R as critical proteins in the regulation of motor neuron survival and cell death. Mutant SOD facilitates Hsp90 nitration, which is known to induce P2X7R mediated cell death, an effect that may explain mutant SOD toxicity. Selective therapeutic targeting of nitrated Hsp90, and not the form of Hsp90 responsible for P2X7R repression, is a potential therapeutic target for drug development for the treatment of ALS. Finally we have provided proof of principle that changes in the administration frequency of riluzole may improve therapeutic efficacy of the drug. We have provided significant advances in causality of ALS and new therapeutic approaches.

APPENDIX A: FIGURES

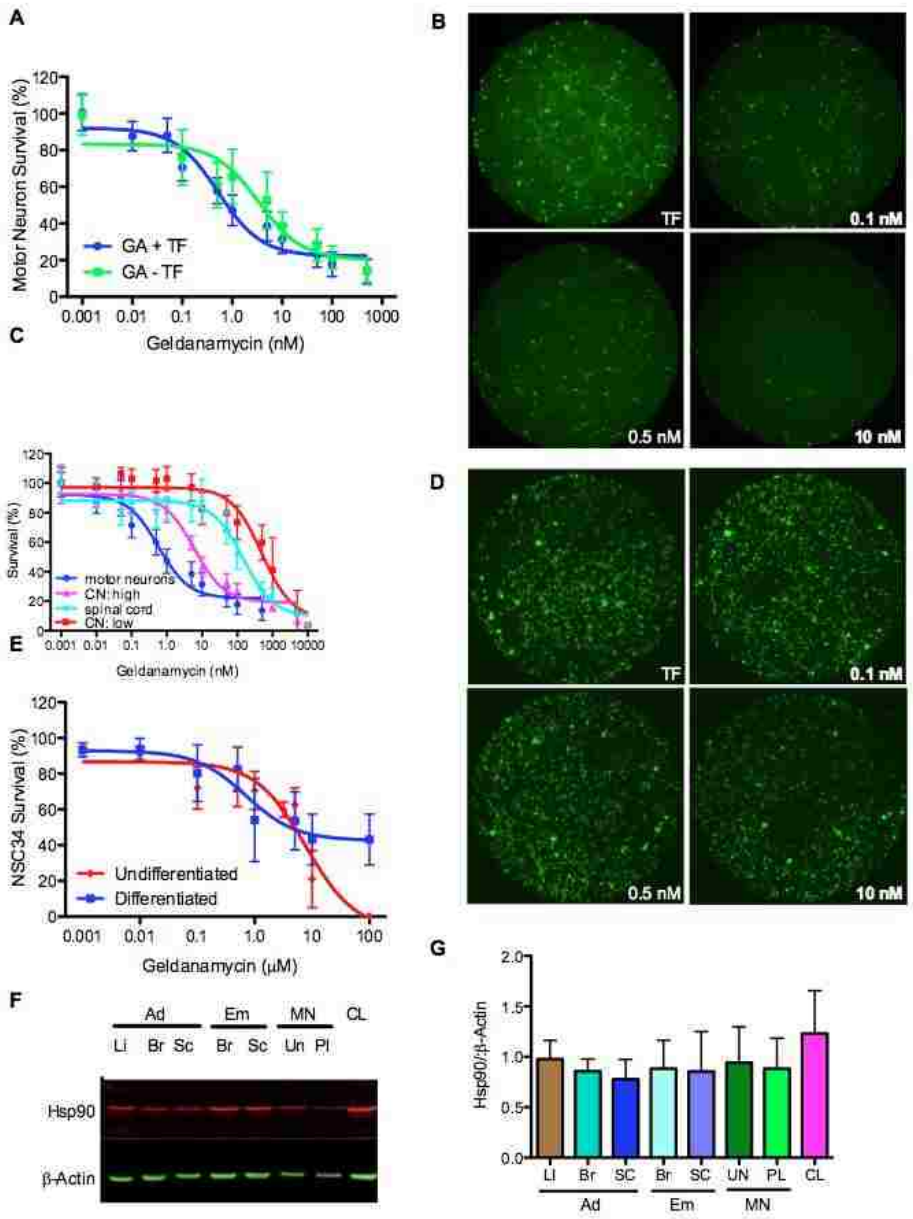

Figure 1: Effect of Hsp90 inhibition on neuronal survival.

Cells were plated in the presence or absence of trophic factors for 24 h prior to geldanamycin treatment. Cell survival was measured using calcein-AM staining. (A) Motor neurons were treated with geldanamycin (GA, 0.01 nM - 500 nM) in the presence (•, +TF) or absence of trophic factors (■, -TF) for 24 h. (B) Representative images of motor neuron cultured in the presence of trophic factors 24 h after addition of geldanamycin (0.1 to 10 nM). The motor neurons were stained with calcein-AM and the images were

captured with a Plate Runner HD (Trophos). (C) Cells from whole embryo ventral spinal cords (◆) and isolated cortical neurons (CN) at high (Δ) or low (■) density were treated with geldanamycin (0.1 nM – 10 uM) for 24 h. (D) Representative images of cortical neurons 24 h after addition of geldanamycin (0.1 to 10 nM). (E) Undifferentiated (◆) and differentiated cells (■) NSC34 cells were treated with geldanamycin (0.1 μM - 100 μM) for 24 h. (F) Levels of Hsp90 were compared in rat tissue including adult liver (Li), adult (Ad) and embryonic (Em) brain (Br), spinal cord (Sc), plated (Pl) and unplated (UN) motor neurons (MN) and the NSC34 motor neuron hybrid cell line (CL) by infrared western blot. (G) Quantitation of Hsp90 levels respect to β-actin. (A-C) Data was fit to a sigmoidal curve, $p < 0.0001$. Columns represent the mean ± SD of at least 3 independent experiments.

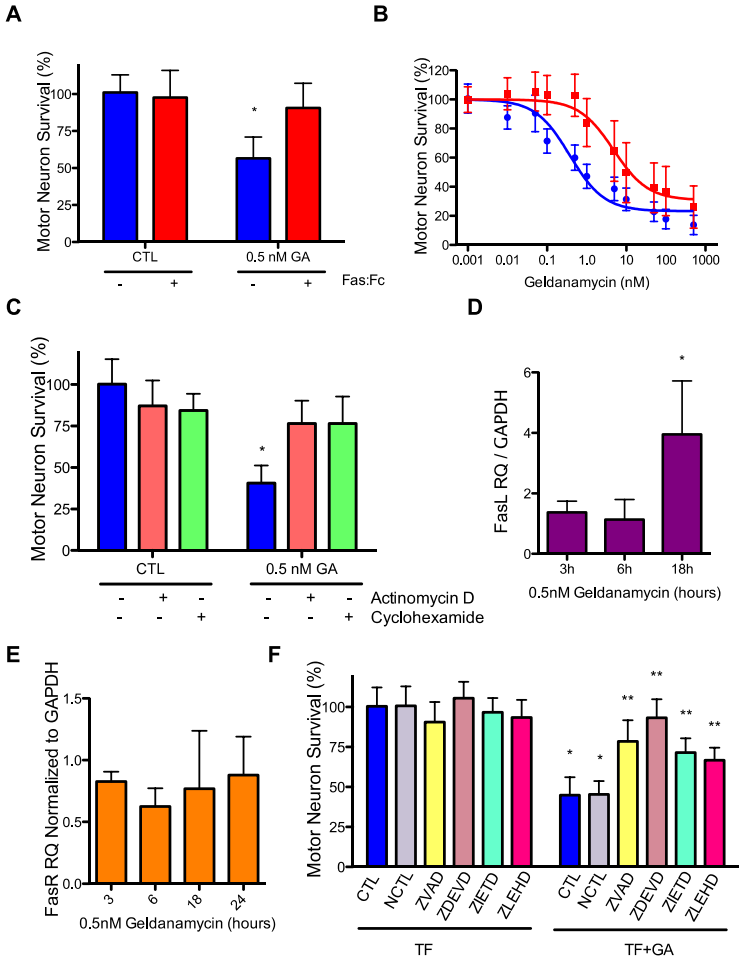

Figure 2: Hsp90 inhibition induces Fas-dependent motor neuron apoptosis.

(A) Cells were treated with 0.5 nM geldanamycin and 1 μg/ml Fas:Fc, and compared to corresponding control (CTL). The data was analyzed using 2-way ANOVA followed by Bonferroni post-hoc test, *$p < 0.05$ versus CTL, **$p < 0.05$ versus CTL+TF. (B) Motor neurons cultured in the presence of trophic factors were treated with geldanamycin (0.01 nM – 500 nM) in the absence (•) or presence of 1 μg/ml Fas:Fc (■) for 24 hours and then stained with Calcein-AM. Data was normalized to control and fit to sigmoidal

curves. The R^2 for the curves was 0.87 for geldanamycin and 0.76 for geldanamycin + Fas:Fc. The EC_{50} values for the curves (0.4 nM and 5nM respectively) were significantly different with $p<0.0001$. **(**C) Motor neurons were treated with 0.5 nM geldanamycin and either 10 μg/ml actinomycin D or 10 μg/ml cycloheximide for 24 h. Motor neuron survival was assessed by calcein-AM staining and normalized to the control (CTL). *$p < 0.05$ versus control by 2-way ANOVA followed by Bonferroni post-hoc test. (D, E) Quantitative RT-PCR for Fas L (D) and Fas receptor (E) normalized to β-actin. Messenger RNA was extracted from motor neurons treated with 0.5 nM geldanamycin for 18 h. Expressed as relative expression to untreated control (n=3). *$p < 0.05$ versus control by 1-way ANOVA followed by Bonferroni post-hoc test. (F) Motor neurons were treated with 0.5 nM geldanamycin and 50 μM of the following caspase inhibitors: NCTL (negative control), Z-VAD (pan), Z-DEVD (caspase 3), Z-IETD (caspase 8), and Z-LEHD (caspase 9) and compared to corresponding control (CTL). Motor neuron survival was assessed by calcein-AM staining and normalized to the control. Statistical analysis was performed using 2-way ANOVA followed by Bonferroni post-hoc test, *$p < 0.05$ versus CTL, **$p<0.05$ versus TF+GA CTL. Columns represent the mean ± SD of at least 3 independent experiments.

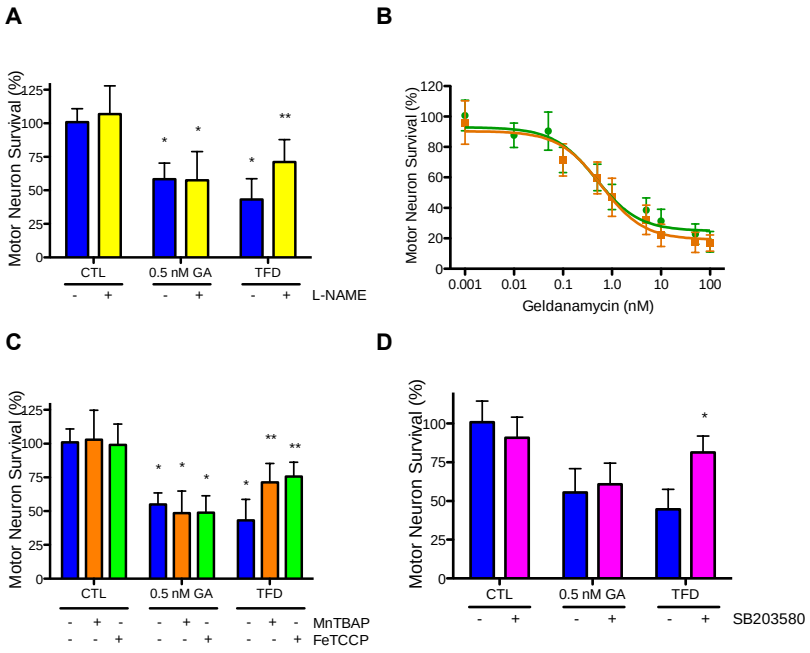

Figure 3: Geldanamycin (GA) induced cell death is independent of oxidative stress.

Motor neurons were cultured in the presence of trophic factors and 0.5 nM geldanamycin or in media without trophic factors (TFD, positive control) and in the presence or absence of either 100 μM L-NAME (A), 50 μM MnTBAP or 50 μM FeTCPP (C), or 5 μM of the p38 MAPK inhibitor SB203580 (D) for 24 h. (B) Motor neurons were cultured in the presence of trophic factors and geldanamycin (0.001-100 nM) and in the absence (•) or presence (■) of 20 μM DETANONOate for 24 h. Data was fit to a sigmoidal curve, and values represent the mean ± 95% CI. Motor neuron survival was assessed by calcein-AM staining and normalized to control. Statistical analysis was performed using 2-way ANOVA followed by Bonferroni post-hoc test, *$p<0.05$ versus control, **$p<0.001$ versus TFD. Columns represent the mean ± SD of at least 3 independent experiments.

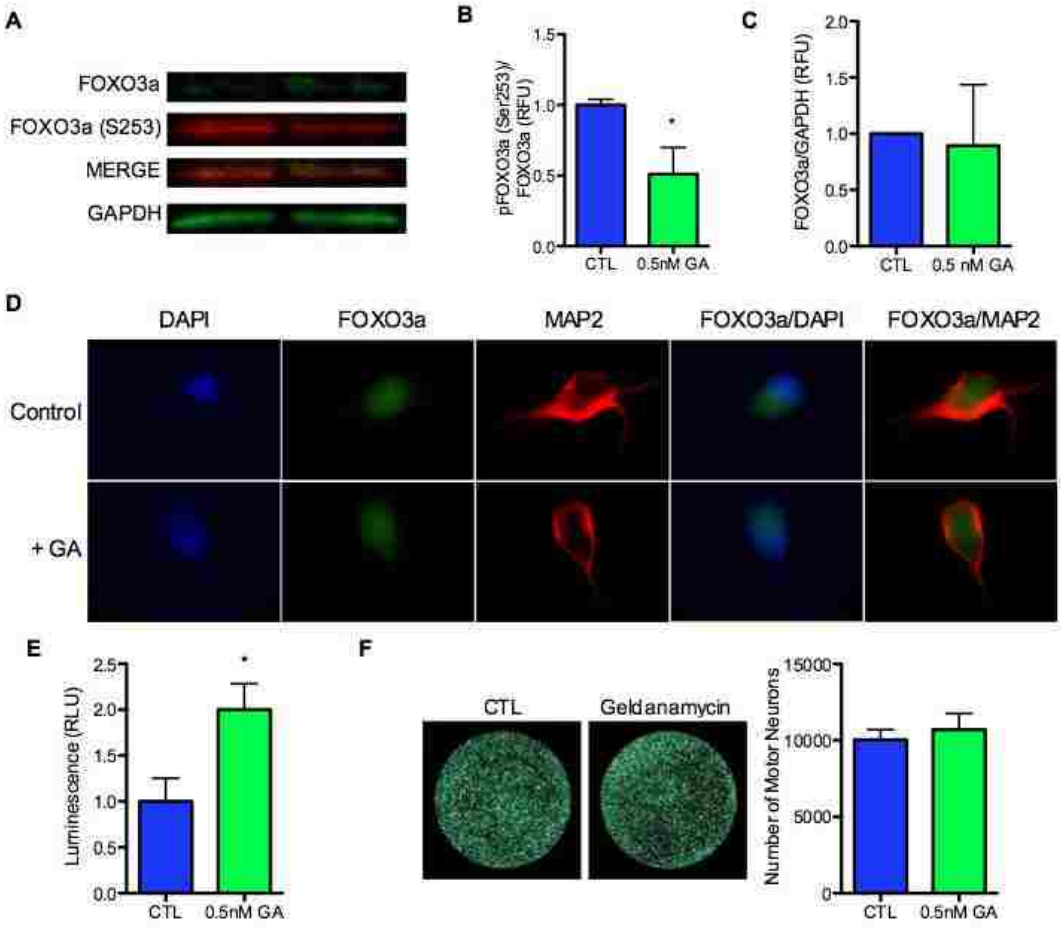

Figure 4: Inhibition of Hsp90 induces FOXO3a transcription factor activation and nuclear translocation.

(A) Representative infrared western blot for total Foxo3a and phosphorylated FOXO3a(S253) from motor neurons treated with 0.5 nM geldanamycin (GA) for 16 hours. Band intensity was quantified and ratios of FOXO3a(Ser253) versus total FOXO3a (B) and FOXO3a versus GAPDH (C) were calculated. (D) Representative inmmunofluorescence of motor neurons transduced with an adenoviral vector expressing FOXO3a. Cells were cultured for 72 h and then cultured in the presence of 0.5 nM geldanamycin for additional 16 h. (E-G) Motor neurons were transduced with lentiviral particles expressing luciferase under the control of fork head response element (FHRE) for 24 h. Cells were then cultured with 0.5 nM geldanamycin for 16 h prior to assessing luciferase activity (E) and motor neuron survival with calcein-AM staining (F). Columns represent the mean ± SD of at least 3 independent experiments. Statistical analysis was performed using a student t-test, *$p < 0.05$ vs CTL.

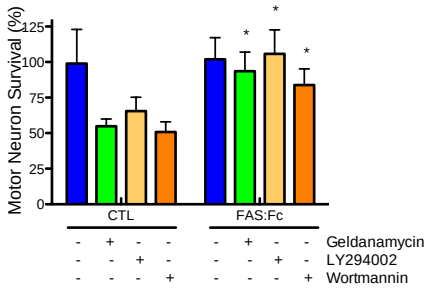

Figure 5: Inhibition of PI3K/AKT pathway induces cell death via FAS.

Motor neurons were treated with either 10 μM LY294002, 10 μM Wortmannin or 0.5 nM geldanamycin in the presence or absence of Fas:Fc for 24 hours and stained with Calcein-AM. Data was normalized to the corresponding control (CTL). Values are the mean ± SD of at least 3 independent experiments performed by triplicate. The results were analyzed using 2-way ANOVA followed by Bonferroni multiple comparison test. *p<0.001 versus control.

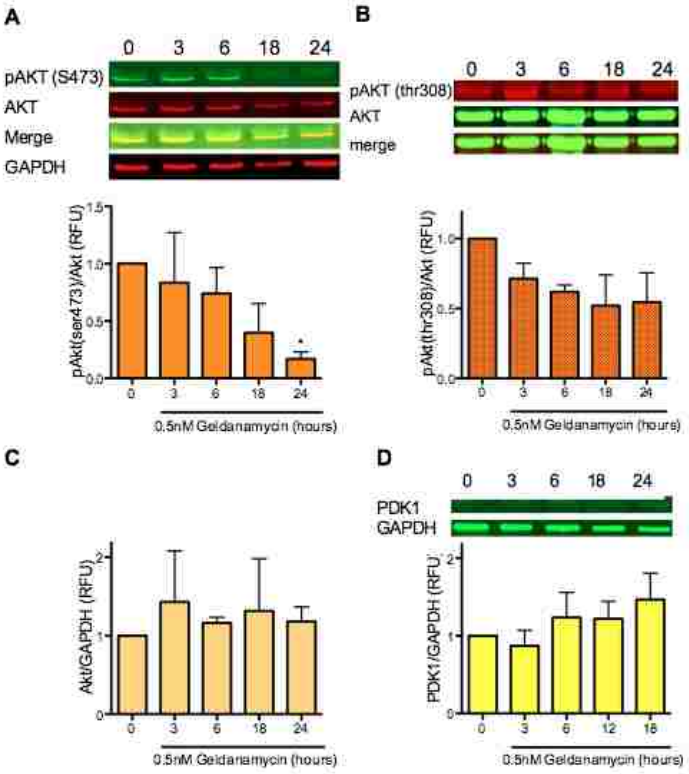

Figure 6: Hsp90 inhibition reduces AKT phosphorylation.

(A-D) Representative infrared western blots for total Akt, phospho-Akt(Ser 473), phospho-Akt(Thr 308), PDK1 and GAPDH from motor neurons treated with 0.5 nM geldanamycin for 24 h. Band intensity was quantified and ratios of pAkt(Ser473) vs. total Akt (A), pAkt(Thr308) vs. total Akt (B), total Akt vs. GAPDH (C), and PDK1 vs. GAPDH (D) were calculated. Values are the mean ± SD of at least 3 independent experiments. Results were analyzed by 1-way ANOVA followed by Bonferroni post-hoc test. *p<0.05 versus respective control.

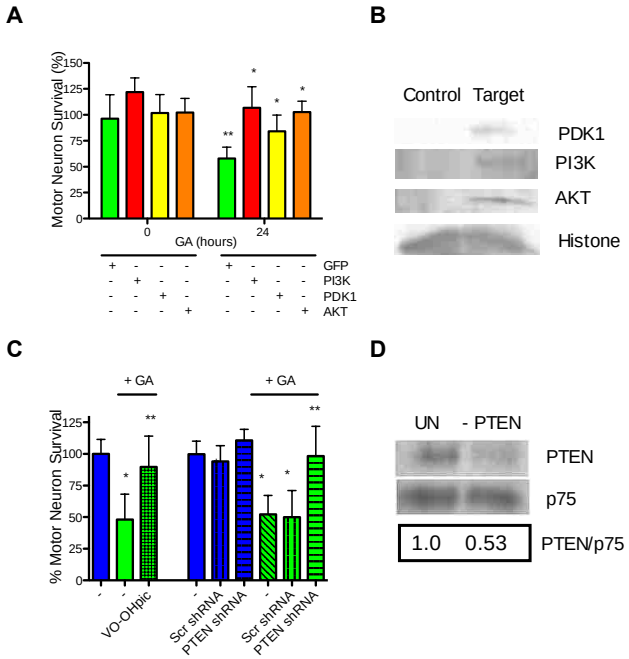

Figure 7: Hsp90 inhibition induces apoptosis by PTEN mediated inhibition of the PI3K/AKT pathway.

(A) Motor neurons were transduced with adenoviral vectors expressing GFP alone, or co-expressing GFP and either constitutive active PI3K, PDK1 or constitutive active Akt. Seventy-two hours later GFP positive cells were counted (t=0) prior to media replacement with either 0.5 nM geldanamycin (GA) or trophic factors alone for additional 24 h. Data was normalized to t=0. Values are the mean ± SD of at least 3 independent experiments performed by quadruplicate. Results were analyzed by 2-way ANOVA followed by Bonferroni post-hoc test. *p < 0.001 versus GA-treated GFP, **p < 0.05 versus GFP. (B) Expression of the recombinant proteins PI3K, PDK1 and Akt was confirmed by infrared western blot for myc-tag. (C) Motor neurons were incubated with 0.5 nM geldanamycin for 24 h in the absence or presence of the PTEN inhibitor, VO-OH(pic) (VOOH, 2 **μ**M) or 48 h after transducing with PTEN or scrambled shRNA lentiviral particles. Cells were counted and normalized to control. *p < 0.05 versus respective control, **p<0.05 versus respective control+GA by 1-way ANOVA followed by Bonferroni post-hoc test. (D) Downregulation of PTEN expression by PTEN shRNA was confirmed by infrared western blot 48 h after motor neuron transduction and normalized to p75 receptor. Columns represent the mean ± SD of at least 3 independent experiments.

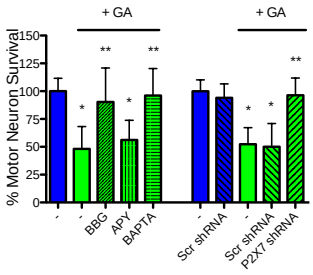

Figure 8: Hsp90 inhibition activates P2X7 receptor.

Motor neurons were incubated with 0.5 nM geldanamycin (GA) in the absence or presence of either P2X7 inhibitor Brilliant Blue G (BBG, 10 μM), apyrase (APY, 1 U/mL) or the calcium chealator BAPTA-AM (1 μM) for 24 h (left). Alternatively, cells were transduced with P2X7 receptor or scrambled shRNA lentiviral particles for 48 h and then cultured in the presence of 0.5 nM geldanamycin for additional 24 h (right). Survival was assessed by calcein-AM staining and normalized to control. *$p < 0.05$ versus GA by 1-way ANOVA followed by Bonferroni post-hoc test. Columns represent the mean ± SD of at least 3 independent experiments.

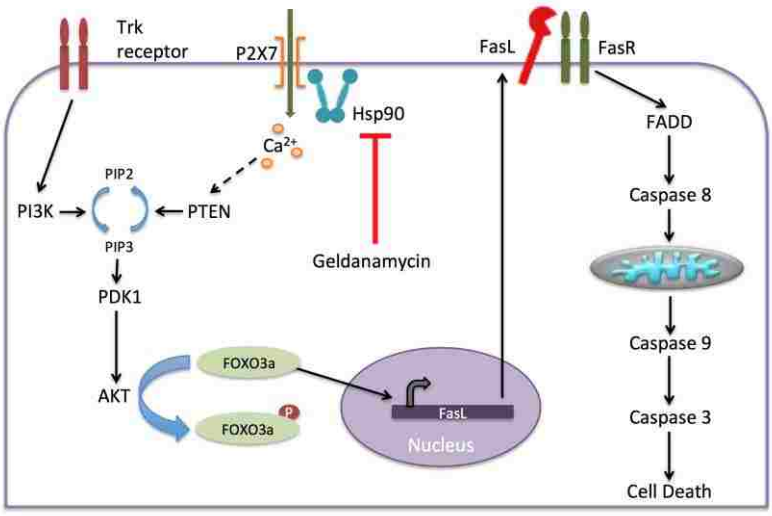

Figure 9: Inhibition of Hsp90 induces motor neuron cell death via P2X7/PTEN dependent pathway.

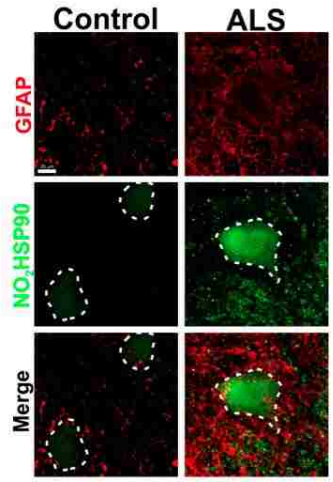

Figure 10: Spinal motor neurons of ALS patients contain NO_2Hsp90

Transverse section of post mortem spinal cord from control and ALS patient immunostained for glial fibrillary acidic protein (GFAP, red) and nitrated Hsp90 (NO_2Hsp90, green). Images were obtained using confocal microscopy. Dotted lines correspond to motor neurons.

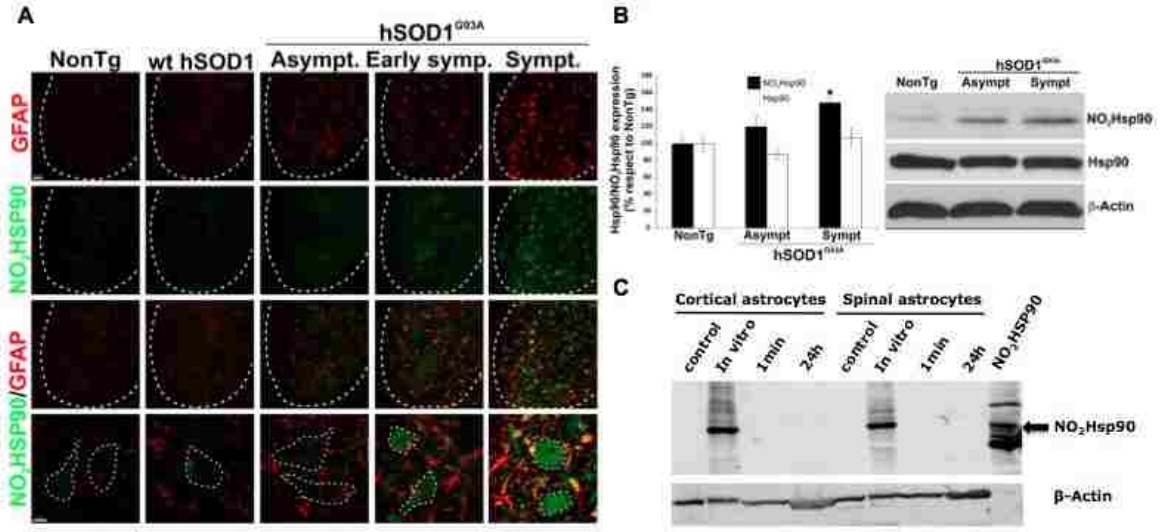

Figure 11: NO_2Hsp90 is detected in G93A mice spinal cord during symptomatic phase.

(A) Nontransgenic (NonTg), wild type SOD transgenic (wt hSOD1), asymptomatic (p60), early symptomatic (p90), and symptomatic (p120) mutant G93A transgenic animals ($hSOD1^{G93A}$) were transcardial perfused. 30-40 μm transverse sections of ventral spinal cord were immunostained for glial fibrillary acidic protein (GFAP, red) and nitrated Hsp90 (NO_2Hsp90, green) and imaged using confocal microscopy (dotted lines). (B) Spinal cord homogenate (40 μg) was separated by SDS-PAGE and immunoblotted for nitrated Hsp90 (NO_2Hsp90) and Hsp90. Band intensities were quantified and normalize to B-actin. (C) Cortical and spinal astrocytes were treated with peroxynitrite for 1 min and 24 hours. Cell lysate were then prepared and separated by SDS-PAGE and immuoblotted for NO_2Hsp90 and β-actin. Peroxynitrite-treated cell lysate (in vitro) was included as a control.

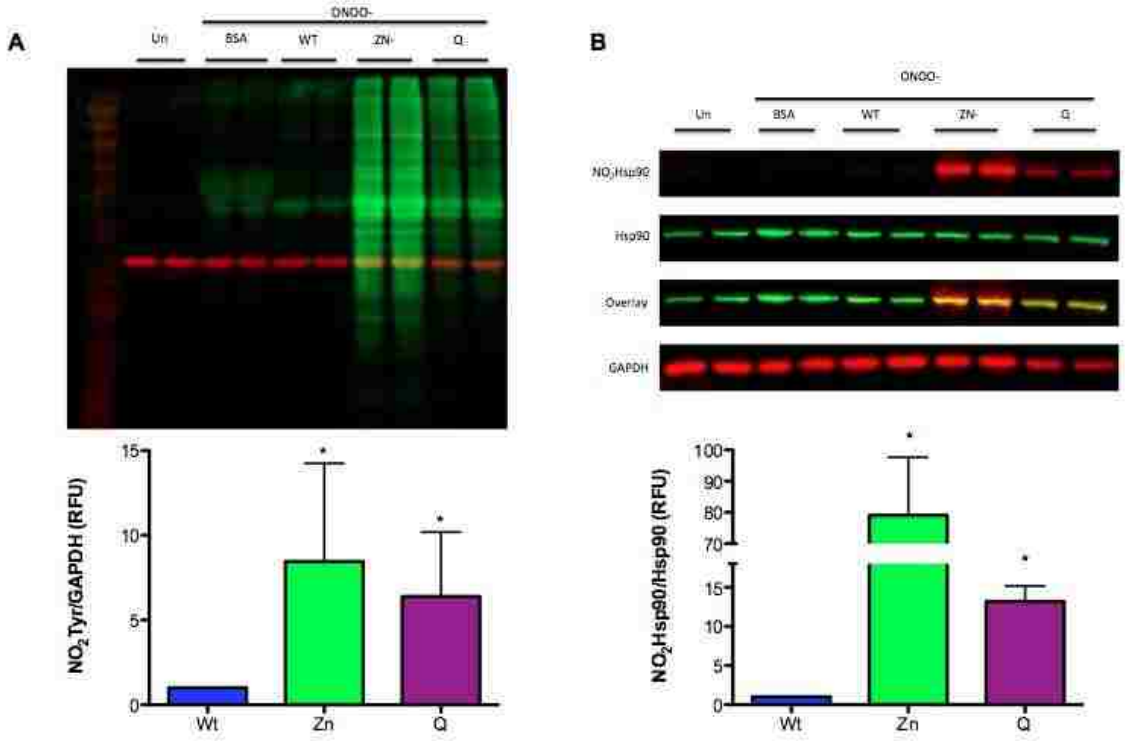

Figure 12: Zinc deficient and Quad mutant SOD.

Peroxynitrite (0.5 mM) was added to brain homogenate (1 mg/ml) in the presence or absence of either wild type (Wt, blue), zinc deficient (Zn-, green) or quad (Q, purple) SOD (1 mg/mL). Following brief vortexing, samples were separated on a SDS-PAGE and immunoblotted for nitrotyrosine (NO_2Tyr, green), nitrated Hsp90 (NO_2Hsp90, red), Hsp90 (green) and GAPDH (red). (A) Lane intensity of NO_2Tyr was normalized to GAPDH and (B) band intensity of NO_2Hsp90 was normalized to Hsp90. Statistical analysis was performed using 1-way ANOVA followed by Bonferroni multiple comparison's test. * $p<0.05$ vs Wt.

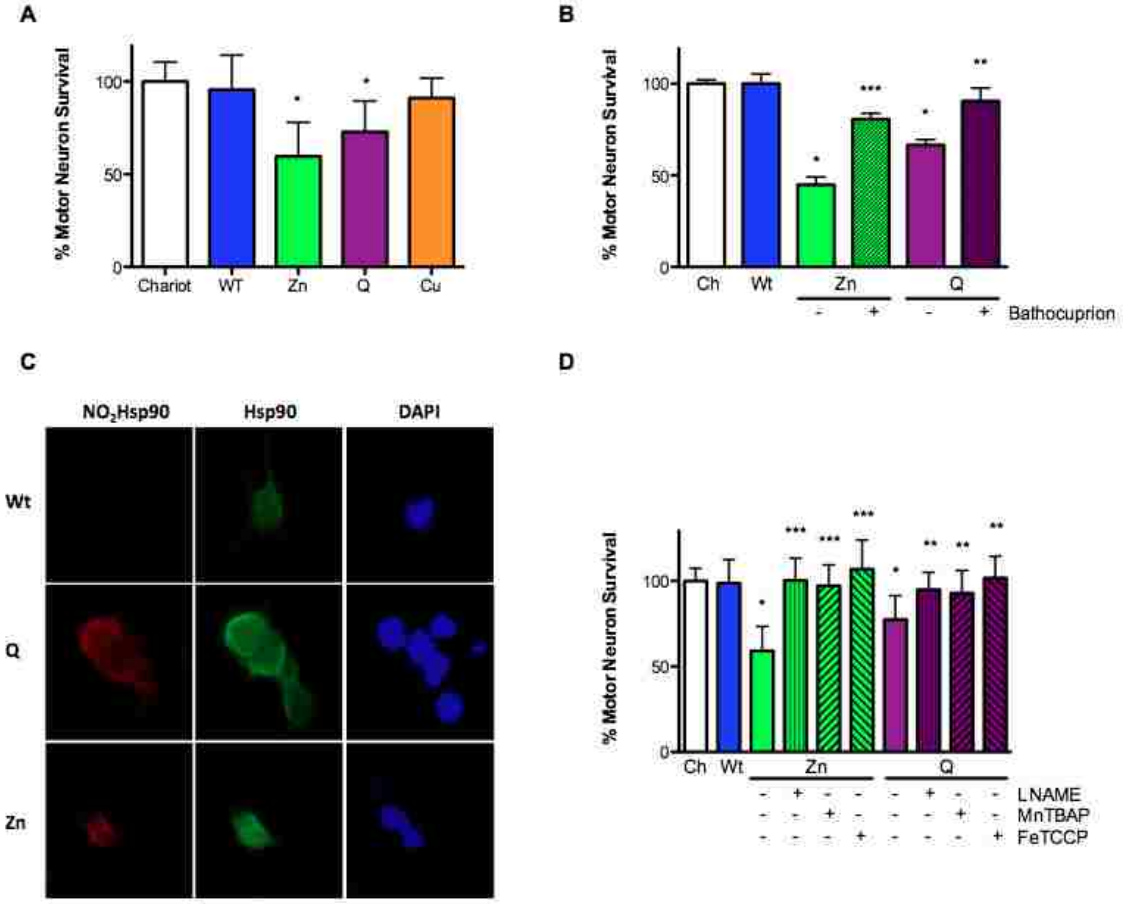

Figure 13: Quad mutant SOD-induced motor neuron death requires copper-mediated oxidative signaling.

(A and B) Wild type (Wt, blue), zinc deficient (Zn, green), quad mutant (Q, purple) and copper deficient (Cu) SOD was delivered to motor neurons using the cell permeant agent chariot in the absence (A) or presence (B) of 50 μM bathocuprione. After 24 h in culture motor neurons were counted by hand or stained using Calcein AM. Data normalized to chariot control. Statistical analysis was performed using one way ANOVA followed by Bonferroni multiple comparison's test. * $p<0.05$ vs Wt. ** $p<0.05$ vs Q. *** $p<0.05$ vs Zn. (C) Motor neurons were fixed 16 h following Wt, Zn, and Q SOD intracellular delivery and immunostained for NO_2Hsp90 (red) and Hsp90 (green). DAPI was used as nuclear staining. (D) Motor neurons were treated as described in A in the presence or absence of 100 μM L-NAME, 50 μM FeTCPP, or 50 μM MnTBAP immediately following chariot delivery. After 24 h in culture motor neurons were counted by hand or stained using Calcein AM. Data normalized to chariot control. Statistical analysis was performed using one way ANOVA followed by Bonferroni multiple comparison's test. * $p<0.05$ vs Wt. ** $p<0.05$ vs Q. *** $p<0.05$ vs Zn.

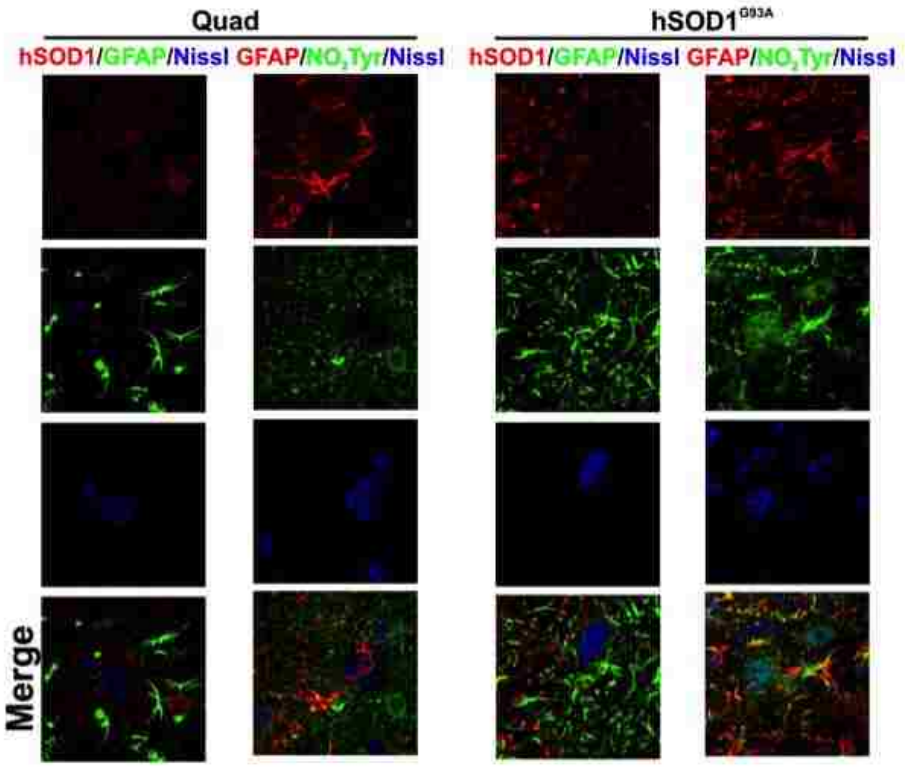

Figure 14: Nitrotyrosine is detected in spinal cord from Quad mutant SOD transgenic mice.

Quad and G93A transgenic mice were transcardial perfused. 30-40 μm transverse ventral spinal cord sections were immunostained for human SOD (hSOD), glial fibrillary acidic protein (GFAP), nitrotyrosine (NO_2Tyr, green) and Nissl (blue) and imaged using confocal microscopy.

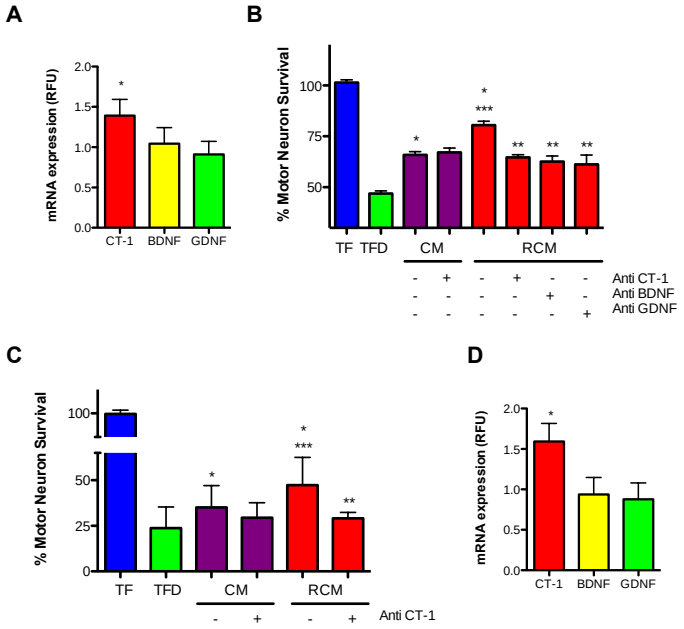

Figure 15: Riluzole induces cardiotrophin-1 production in astrocytes and Schwann cells.

Confluent astrocytes (A) were treated with riluzole for 24 h, RNA was extracted and the levels of CT-1, BDNF and GDNF were quantified, normalized against β-actin and expressed as relative levels respect to untreated cells. Conditioned media from astrocytes (B) and Schwann cells (C) was obtained by incubating the cells in the presence or absence of riluzole for 24 h, replacing the media and leaving the cells to condition the fresh media in the absence of riluzole for additional 24 h. Motor neurons were plated in the presence of the trophic factors BDNF, GDNF, and CT-1 (TF) or in the absence of trophic factors (trophic factor deprivation, TFD). When indicated, trophic factor-deprived motor neurons were plated in the presence of 1/10 dilution (A) or 1/25 dilution (C) of either untreated conditioned media (CM) or riluzole-conditioned media (RCM) and in the presence or absence of neutralizing antibody against CT-1 (Anti CT-1), BDNF (Anti BDNF) and GDNF (Anti GDNF). Motor neurons were cultured for 3 d then counted by hand or using Calcein AM. Confluent Schwann cells (D) were treated with riluzole for 24 h, RNA was extracted and the levels of CT-1, BDNF and GDNF were quantified as described in A. Values are the mean of at least 3 experiments. For B and C, *p<0.05 vs TFD, **p<0.05 vs RCM, *** p<0.05 vs CM. For A and D, *p<0.05 vs BDNF or GDNF. Statistical analysis was performed using one-way ANOVA followed by Bonferroni post-test.

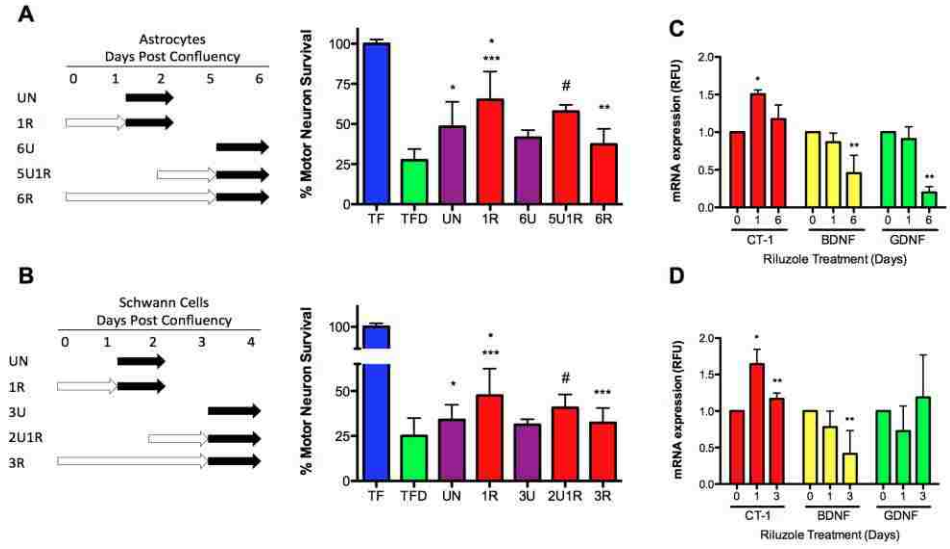

Figure 16: Chronic riluzole treatment reduces trophic factor production in astrocytes and Schwann cells.

Motor neurons were plated in the presence (TF) or absence of trophic factors (TFD), or with media conditioned by astrocytes (A) or Schwann cells (B) for the indicated periods of time (white arrows). Riluzole was then replaced with new media without riluzole and 24 h later conditioned media was collected (black arrows). (A) Motor neurons were plated with conditioned media from astrocytes cultured in the absence of riluzole for one (UN) or 6 days (6U) or presence of riluzole for 24 h (1R) or 6 days (6R), or cultured for 5 days prior to 24 h incubation with riluzole (5U1R). Motor neurons were cultured for 3 days in the conditioned media then counted by hand or using Calcein AM. (B) Motor neurons were plated in conditioned media from Schwann cells and cultured in the absence of riluzole for one day (UN) or 3 days (3U) or presence of riluzole for 24 h (1R), 3 days (3R), and for 2 days and then treated with riluzole for 24 h (2U1R). Motor neurons were cultured for 3 days in described conditioned media then counted by hand or using Calcein AM. (C) Astrocytes were incubated without (0) or with riluzole for 24 h (1) and 6 days (6) before RNA was extracted. The relative changes in mRNA expression of CT-1 (red) BDNF (yellow) and GDNF (green) were determined using β-actin to normalize. (D) Schwann cells were incubated without (0) or with riluzole for 24 h (1) and 3 days (3) before determining the relative changes in mRNA expression of CT-1 (red) BDNF (yellow) and GDNF (green) were determined as described in C. Values are the mean ± SD of at least 3 independent experiments. For A and B, statistical analysis was performed using ANOVA followed by Bonferroni multiple comparison's test, *$p<0.05$ vs TFD, **$p<0.05$ vs 1R, *** $p<0.005$ vs UN. # $p<0.05$ vs 6U. For C and D, *$p<0.05$ vs. 0 day riluzole, **$p<0.05$ vs. 1 day riluzole.

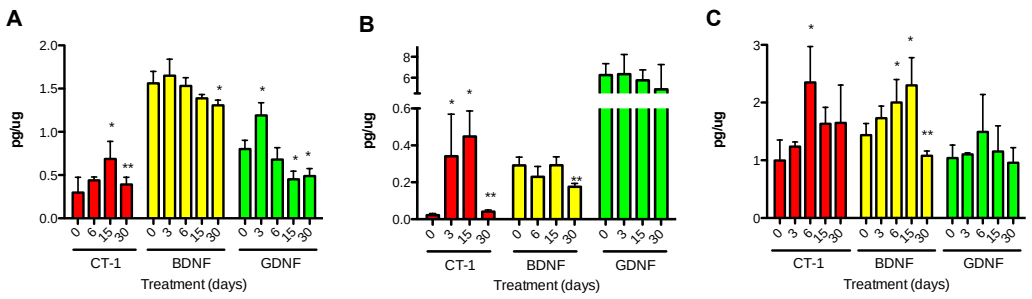

Figure 17: Effects of riluzole on the trophic factor levels in vivo.

Male C57BL/6J mice were treated with riluzole (100 µg/ml) in the drinking water for the periods indicated in the figures. At the indicated times the mice were sacrificed, the tissues harvested and stored at -80°C. Spinal cord (A) sciatic nerve (B) and brain (C) were homogenized and CT-1 (red), GDNF (green) and BDNF (red) protein levels were quantified by ELISA. Values are the mean of at least three animals from at least two independent studies performed by duplicate. Statistical analysis was performed using 1-way ANOVA followed by Bonferroni multiple comparison's test, * $p<0.001$ vs control **$p<0.05$ vs 15 days

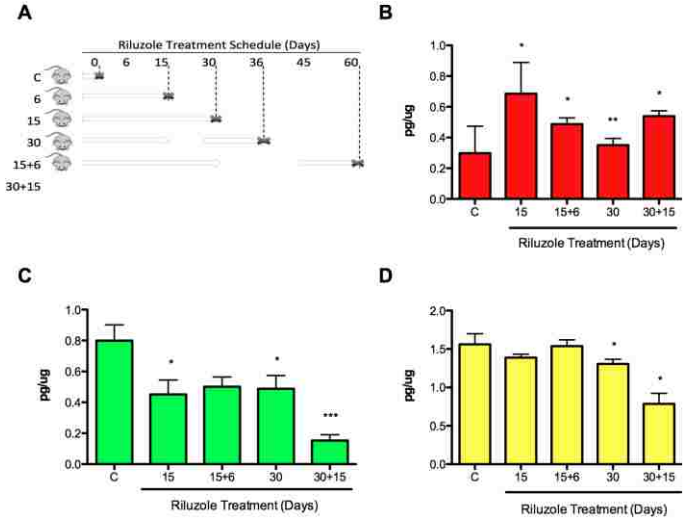

Figure 18: Discontinuous treatment of riluzole maintains higher levels of trophic factors.

(A) Riluzole treatment schedule. Animals were administered riluzole (grey arrows) in their drinking water (100 µg/ml) continuously for 15 or 30 days then riluzole was removed for another 15 days before receiving a second dose of riluzole for additional 6 or 15 days. At the indicated time points the mice were sacrificed (x), the tissues were harvested and stored at -80°C. Spinal cord was homogenized and CT-1 (B), GDNF (C) and BDNF (D) concentrations were quantified by ELISA. Values are the mean of at least 4 mice with

the determinations performed by duplicate. Statistical analysis was performed using ANOVA followed by Bonferroni post-test. * $p<0.001$ vs control **$p<0.05$ vs 15 days, #$p<0.05$ vs 3 days, ## $p<0.05$ vs 30 days.

APPENDIX B: TABLES

Table 1: EC_{50} of different cell types treated with geldanamycin

Cells were treated with geldanamycin (0.01 nM to 100 μM) for 24 hours. Cell survival was measured using calcein-AM staining as described in material and methods. Values represent the mean and 95% CI of at least 3 independent experiments. Data was fit to a sigmoidal curve, $p < 0.0001$.

Cell Type	EC_{50} (95% CI)	Ratio to Motor Neurons + TF	R^2
Motor Neuron +TF	0.5 nM (0.4 nM to 0.6 nM)	1	0.89
Motor Neuron - TF	3.4 nM (2.4 nM to 4.8 nM)	7	0.74
Embryo Ventral Spinal Cord	146 nM (118.3 nM to 180.3 nM)	292	0.84
High Density Cortical Neurons	5.9nM (4.95 nM to 7.1 nM)	12	0.94
Low Density Cortical Neurons	497.6 nM (404.8 nM to 611.7 nM)	995	0.80
NSC34 undifferentiated	7.75 μM (6.1 μM to 9.8 μM)	15500	0.82
NSC34 differentiated	0.70 μM (0.4 μM to 1.2 μM)	1400	0.65

Table 2: Metal deficient SOD binds Hsp90.

Dissociation constants (KD) for wild type (Wt), zinc deficient (Zn), copper deficient (Cu), and copper/zinc deficient SOD (APO) binding to Hsp90 were determined using surface plasmon resonance (SPR). Increasing concentrations of wild type and mutant SOD were passed over immobilized Hsp90 to calculate the KD (nM).

	KD
WT	0.0
Zn	80.5
Cu	75.0
APO C111S	70.3

APPENDIX C: SUPPLEMENTAL FIGURES

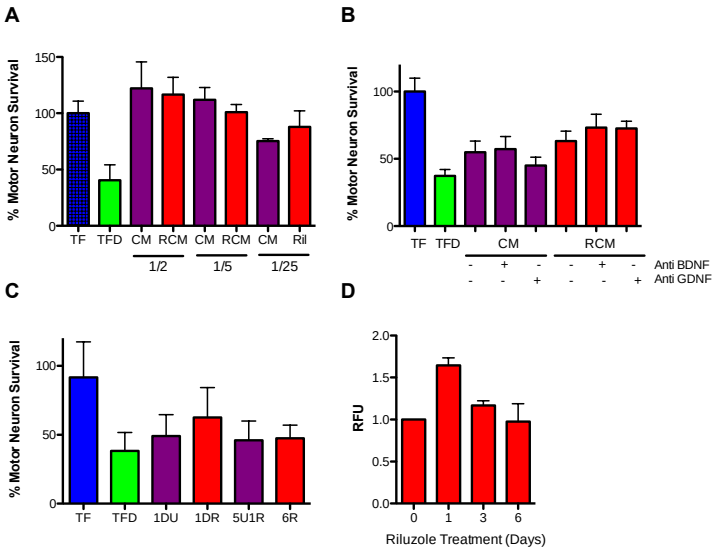

Supplemental Figure 1: Optimization of experiments conducted in Schwann Cells

Conditioned media from Schwann cells (A) was obtained by incubating the cells in the presence or absence of riluzole for 24 h, replacing the media and leaving the cells to condition the fresh media in the absence of riluzole for additional 24 h. Motor neurons were plated in the presence of the trophic factors BDNF, GDNF, and CT-1 (TF) or in the absence of trophic factors (trophic factor deprivation, TFD). When indicated, trophic factor-deprived motor neurons were plated in the presence of indicated dilution of either untreated conditioned media (CM) or riluzole-conditioned media (RCM) for three days. Motor neuron survival was determined by counting by hand. B) Motor neurons were cultured in the presence of a 1/25 dilution of untreated and riluzole treated conditioned media with or without neutralizing antibody against BDNF (Anti BDNF) and GDNF (Anti GDNF). Cells were cultured for 3 d then counted by hand. C) Motor neurons were plated with conditioned media from Schwann cells incubated in absence (UN) or with riluzole for 24 h (1R), 6 days (6R), or cultured for 5 d the before incubation with riluzole for 24 h (5U1RD). D) Schwann cells were treated with riluzole for one, three and six days. RNA was extracted and relative levels of CT-1, BDNF and GDNF were quantified (normalized using β-actin).

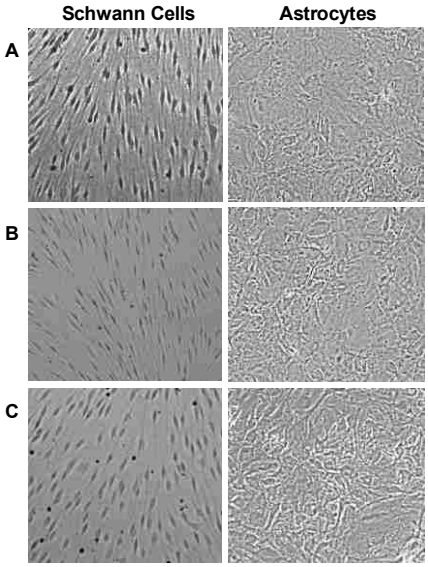

Supplemental Figure 2: Riluzole treatment does not affect cell morphology.

Confluent astrocytes and Schwann cells cultured in the absence (A) or presence of riluzole for 24 h (B) or 3 days for Schwann cells (C) or 6 days for astrocytes (C).

REFERENCES

Abe, K., L. H. Pan, et al. (1995). "Induction of nitrotyrosine-like immunoreactivity in the lower motor neuron of amyotrophic lateral sclerosis." Neurosci. Lett. **199**: 152-154.

Adams, L., M. C. Franco, et al. (2015). "Reactive nitrogen species in cellular signaling." Exp Biol Med (Maywood) **240**(6): 711-717.

Adinolfi, E., M. Kim, et al. (2003). "Tyrosine phosphorylation of HSP90 within the P2X7 receptor complex negatively regulates P2X7 receptors." The Journal of biological chemistry **278**(39): 37344-37351.

Aebischer, J., P. Cassina, et al. (2010). "IFNgamma triggers a LIGHT-dependent selective death of motoneurons contributing to the non-cell-autonomous effects of mutant SOD1." Cell Death Differ **18**(5): 754--768.

Ang, L. C., B. Bhaumick, et al. (1993). "Neurite promoting activity of insulin-like growth factor I and nerve growth factor on spinal motoneurons is astrocyte dependent." Brain Res Dev Brain Res **74**(1): 83-88.

Apolloni, S., S. Amadio, et al. (2014). "Spinal cord pathology is ameliorated by P2X7 antagonism in a SOD1-mutant mouse model of amyotrophic lateral sclerosis." Dis Model Mech **7**(9): 1101-1109.

Arce, V., R. A. Pollock, et al. (1998). "Synergistic effects of schwann- and muscle-derived factors on motoneuron survival involve GDNF and cardiotrophin-1 (CT-1)." J Neurosci **18**(4): 1440-1448.

Barbeito, L., M. Pehar, et al. (2004). "Role of astroglia in the pathogenesis of amyotrophic lateral sclerosis." Brain Res Rev **47**: 263-274.

Barthelemy, C. C., C. E. Henderson, et al. (2004). "Foxo3a induces motoneuron death through the Fas pathway in cooperation with JNK." BMC neuroscience **5**(1): 48.

Basso, A. D., D. B. Solit, et al. (2002). "Akt Forms an Intracellular Complex with Heat Shock Protein 90 (Hsp90) and Cdc37 and Is Destabilized by Inhibitors of Hsp90 Function." J. Biol. Chem. **277**(42): 39858-39866.

Basso, M., S. Pozzi, et al. (2013). "Mutant copper-zinc superoxide dismutase (SOD1) induces protein secretion pathway alterations and exosome release in astrocytes: implications for disease spreading and motor neuron pathology in amyotrophic lateral sclerosis." J Biol Chem **288**(22): 15699-15711.

Batulan, Z., G. A. Shinder, et al. (2003). "High threshold for induction of the stress response in motor neurons is associated with failure to activate HSF1." J Neurosci **23**(13): 5789-5798.

Batulan, Z., D. M. Taylor, et al. (2006). "Induction of multiple heat shock proteins and neuroprotection in a primary culture model of familial amyotrophic lateral sclerosis." Neurobiology of Disease **24**(2): 213-225.

Beal, M. F., L. J. Ferrante, et al. (1997). "Increased 3-nitrotyrosine in both sporadic and familial amyotrophic lateral sclerosis." Ann Neurol **42**: 644-654.

Beckman, J. S., T. W. Beckman, et al. (1990). "Apparent hydroxyl radical production by peroxynitrite: implications for endothelial injury from nitric oxide and superoxide." Proc Natl Acad Sci U S A **87**(4): 1620-1624.

Beckman, J. S., M. Carson, et al. (1993). "ALS, SOD and peroxynitrite." Nature **364**(6438): 584.

Beckman, J. S., A. G. Estévez, et al. (2001). "Superoxide dismutase and the death of motoneurons in ALS." TINS **24**(11): S15-S20.

Beckman, J. S. and W. H. Koppenol (1996). "Nitric oxide, superoxide, and peroxynitrite: the good, the bad, and ugly." Am J Physiol **271**(5 Pt 1): C1424-1437.

Behzad, H., S. Jamil, et al. (2007). "Cytokine-mediated FOXO3a phosphorylation suppresses FasL expression in hemopoietic cell lines: investigations of the role of Fas in apoptosis due to cytokine starvation." Cytokine **38**(2): 74-83.

Bellingham, M. C. (2011). "A review of the neural mechanisms of action and clinical efficiency of riluzole in treating amyotrophic lateral sclerosis: what have we learned in the last decade?" CNS Neurosci Ther **17**(1): 4-31.

Bensimon, G., L. Lacomblez, et al. (1994). "A controlled trial of riluzole in amyotrophic lateral sclerosis. ALS/Riluzole Study Group." The New England journal of medicine **330**(9): 585-591.

Bergerot, A., P. J. Shortland, et al. (2004). "Co-treatment with riluzole and GDNF is necessary for functional recovery after ventral root avulsion injury." Exp Neurol **187**(2): 359-366.

Berthod, F. and F. Gros-Louis (2012). In Vivo and In Vitro Models to Study Amyotrophic Lateral Sclerosis. Amyotrophic Lateral Sclerosis. M. H. Maurer. http://www.intechopen.com/books/amyotrophic-lateral-sclerosis/in-vivo-and-in-vitro-models-to-study-amyotrophic-lateral-sclerosis, InTech.

Boillee, S., K. Yamanaka, et al. (2006). "Onset and Progression in Inherited ALS Determined by Motor Neurons and Microglia." Science **312**(5778): 1389-1392.

Bordet, T., J. C. Lesbordes, et al. (2001). "Protective effects of cardiotrophin-1 adenoviral gene transfer on neuromuscular degeneration in transgenic ALS mice." Hum Mol Genet **10**(18): 1925-1933.

Brockes, J. P., K. L. Fields, et al. (1979). "Studies on cultured rat Schwann cells. I. Establishment of purified populations from cultures of peripheral nerve." Brain Res **165**(1): 105-118.

Bruening, W., J. Roy, et al. (1999). "Up-regulation of protein chaperones preserves viability of cells expressing toxic Cu/Zn-superoxide dismutase mutants associated with amyotrophic lateral sclerosis." J Neurochem **72**(2): 693-699.

Bruijn, L. I., M. F. Beal, et al. (1997). "Elevated free nitrotyrosine levels, but not protein-bound nitrotyrosine or hydroxyl radicals, throughout amyotrophic lateral sclerosis (ALS)-like disease implicate tyrosine

nitration as an aberrant in vivo property of one familial ALS-linked superoxide dismutase 1 mutant." Proc Natl Acad Sci USA **94**: 7606-7611.

Bruijn, L. I., M. W. Becher, et al. (1997). "ALS-Linked SOD1 Mutant G85R Mediates Damage to Astrocytes and Promotes Rapidly Progressive Disease with SOD1-Containing Inclusions." Neuron **18**(2): 327-338.

Bruijn LI, B. M., Lee MK, Anderson KL, Jenkins NA, Copeland NG, Sisodia SS, Rothstein JD, Borchelt DR, Price DL, Cleveland DW. (1997). "ALS-linked SOD1 mutant G85R mediates damage to astrocytes and promotes rapidly progressive disease with SOD1-containing inclusions." Neuron **18**(2): 327-338.

Bruijn, L. I., M. K. Houseweart, et al. (1998). "Aggregation and Motor Neuron Toxicity of an ALS-Linked SOD1 Mutant Independent from Wild-Type SOD1." Science **281**: 1851-1854.

Brunet, A., A. Bonni, et al. (1999). "Akt promotes cell survival by phosphorylating and inhibiting a Forkhead transcription factor." Cell **96**(6): 857-868.

Casoni, F., M. Basso, et al. (2005). "Protein nitration in a mouse model of familial amyotrophic lateral sclerosis: possible multifunctional role in the pathogenesis." J Biol Chem **280**(16): 16295-16304.

Cheah, B. C., S. Vucic, et al. (2010). "Riluzole, neuroprotection and amyotrophic lateral sclerosis." Current medicinal chemistry **17**(18): 1942-1199.

Cifra, A., G. L. Mazzone, et al. (2013). "Riluzole: what it does to spinal and brainstem neurons and how it does it." Neuroscientist **19**(2): 137-144.

Clement, A. M., M. D. Nguyen, et al. (2003). "Wild-type nonneuronal cells extend survival of SOD1 mutant motor neurons in ALS mice." Science **302**(5642): 113-117.

Crow, J. P., J. B. Sampson, et al. (1997). "Decreased zinc affinity of amyotrophic lateral sclerosis-associated superoxide dismutase mutants leads to enhanced catalysis of tyrosine nitration by peroxynitrite." J. Neurochem. **69**(4): 1936-1944.

Crow, J. P., M. J. Strong, et al. (1997). "Superoxide dimutase catalyzes nitration of tyrosines by peroxinitrite in the rod and head domains of neurofilament L." J Neurochem **69**(5): 1945-1953.

Deng, H.-X., Y. Shi, et al. (2006). "Conversion to the amyotrophic lateral sclerosis phenotype is associated with intermolecular linked insoluble aggregates of SOD1 in mitochondria." PNAS **103**(18): 7142-7147.

Deng, H. X., A. Hentati, et al. (1993). "Amyotrophic lateral sclerosis and structural defects in Cu,Zn superoxide dismutase." Science **261**(5124): 1047-1051.

Dennys, C. N., J. Armstrong, et al. (2015). "Chronic inhibitory effect of riluzole on trophic factor production." Exp Neurol. 271:301-307.

Dennys, C. N., M. C. Franco, et al. (2014). "Trophic factor production by glial cells in the treatment of amyotrophic lateral sclerosis." J Biomed Eng **1**(5): 8.

Diaz-Amarilla, P., S. Olivera-Bravo, et al. (2011). "Phenotypically aberrant astrocytes that promote motoneuron damage in a model of inherited amyotrophic lateral sclerosis." Proceedings of the National Academy of Sciences of the United States of America **108**(44): 18126-18131.

Didelot, C., E. Schmitt, et al. (2006). Heat shock proteins: endogenous modulators of apoptotic cell death. Molecular Chaperones in Health and Disease. M. Gaestel. Berlin, Springer. **172:** 171-198.

Doble, A. (1997). "Effects of riluzole on glutamatergic neurotransmission in the mammalian central nervous system, and other pharmacological effects." Reviews in Comtemporary Pharmacology **8**: 213-225.

Dolcet, X., J. Egea, et al. (1999). "Activation of phosphatidylinositol 3-kinase, but not extracellular-regulated kinases, is necesary to mediate brain-derived neurotrophic factor-induced motoneuron survival." J Neurochem **73**: 521-531.

Dougherty, K. D., C. F. Dreyfus, et al. (2000). "Brain-derived neurotrophic factor in astrocytes, oligodendrocytes, and microglia/macrophages after spinal cord injury." Neurobiol Dis **7**(6 Pt B): 574-585.

Duda, J. E., B. I. Giasson, et al. (2000). "Widespread nitration of pathological inclusions in neurodegenerative synucleinopathies." Am. J. Pathol. **157**(5): 1439-1445.

Dulin, J. N., M. L. Moore, et al. (2013). "The dual cyclooxygenase/5-lipoxygenase inhibitor licofelone attenuates p-glycoprotein-mediated drug resistance in the injured spinal cord." J Neurotrauma **30**(3): 211-226.

Eagleson, K. L. and M. R. Bennett (1986). "Motoneurone survival requirements during development: the change from immature astrocyte dependence to myotube dependence." Developmental Brain Research **29**(2): 161-172.

Eagleson, K. L., T. R. Raju, et al. (1985). "Motoneuron survival is induced by immature astrocytes from developing avian spinal cord." Dev Brain Res **17**: 95-104.

Estévez, A. G., J. P. Crow, et al. (1999). "Induction of nitric oxide-dependent apoptosis in motor neurons by zinc-deficient superoxide dismutase." Science **286**: 2498-2500.

Estevez, A. G., J. B. Sampson, et al. (2000). "Liposome-delivered superoxide dismutase prevents nitric oxide-dependent motor neuron death induced by trophic factor withdrawal." Free Radic Biol Med **28**(3): 437-446.

Estevez, A. G., N. Spear, et al. (1998). "Nitric oxide and superoxide contribute to motor neuron apoptosis induced by trophic factor deprivation." J Neurosci **18**(3): 923-931.

Estevez, A. G., J.-M. Stutzmann, et al. (1995). "Protective effect of riluzole on excitatory amino acid-mediated neurotoxicity in motoneuron-enriched cultures." European Journal of Pharmacology **280**(1): 47-53.

Ferrante, R. J., L. A. Shinobu, et al. (1997). "Increased 3-nitrotyrosine and oxidative damage in mice with a human copper/zinc superoxide dismutase mutation." Ann Neurol **42**: 326-334.

Fiskus, W., R. Rao, et al. (2008). "Molecular and biologic characterization and drug sensitivity of pan-histone deacetylase inhibitor-resistant acute myeloid leukemia cells." Blood **112**(7): 2896-2905.

Foerster, B. R., M. G. Pomper, et al. (2013). "An imbalance between excitatory and inhibitory neurotransmitters in amyotrophic lateral sclerosis revealed by use of 3-T proton magnetic resonance spectroscopy." JAMA Neurol **70**(8): 1009-1016.

Franco, M. C., Y. Ye, et al. (2013). "Nitration of Hsp90 induces cell death." Proc Natl Acad Sci U S A **110**(12): E1102-1111.

Fujita, N., S. Sato, et al. (2002). "Involvement of Hsp90 in Signaling and Stability of 3-Phosphoinositide-dependent Kinase-1." J. Biol. Chem. **277**(12): 10346-10353.

Fulmer, C. G., M. W. VonDran, et al. (2014). "Astrocyte-derived BDNF supports myelin protein synthesis after cuprizone-induced demyelination." J Neurosci **34**(24): 8186-8196.

Gaestel, M. (2006). "Molecular chaperones in signal transduction." Handbook of Experimental Pharmacology **172**: 93-109.

Gandelman, M., M. Levy, et al. (2013). "P2X7 receptor-induced death of motor neurons by a peroxynitrite/FAS-dependent pathway." J Neurochem **126**(3): 382-388.

Garces, A., G. Haase, et al. (2000). "GFRalpha 1 is required for development of distinct subpopulations of motoneuron." J Neurosci **20**(13): 4992-5000.

Ghalali, A., F. Wiklund, et al. (2014). "Atorvastatin prevents ATP-driven invasiveness via P2X7 and EHBP1 signaling in PTEN-expressing prostate cancer cells." Carcinogenesis **35**(7): 1547-1555.

Gifondorwa, D. J., M. B. Robinson, et al. (2007). "Exogenous Delivery of Heat Shock Protein 70 Increases Lifespan in a Mouse Model of Amyotrophic Lateral Sclerosis." J. Neurosci. **27**(48): 13173-13180.

Gonzalez-Zulueta, M., L. M. Ensz, et al. (1998). "Manganese superoxide dismutase protects nNOS neurons from NMDA and nitric oxide-mediated neurotoxicity." J Neurosci **18**(6): 2040-2055.

Gould, T. W. and R. W. Oppenheim (2011). "Motor neuron trophic factors: therapeutic use in ALS?" Brain Res Rev **67**(1-2): 1-39.

Group, A. C. T. S. (1996). "A double-blind placebo-controlled clinical trial of subcutaneous recombinant human ciliary neurotrophic factor (rHCNTF) in amyotrophic lateral sclerosis. ALS CNTF Treatment Study Group." Neurology **46**(5): 1244-1249.

Gurney, M. E., F. B. Cutting, et al. (1996). "Benefit of vitamin E, riluzole, and gabapentin in a transgenic model of familial amyotrophic lateral sclerosis." Ann Neurol **39**(2): 147-157.

Gurney, M. E., T. J. Fleck, et al. (1998). "Riluzole preserves motor function in a transgenic model of familial amyotrophic lateral sclerosis." Neurology **50**(1): 62-66.

Gurney, M. E., H. Pu, et al. (1994). "Motor neuron degeneration in mice that express a human Cu,Zn superoxide dismutase mutation." Science **264**(5166): 1772-1775.

Hall, E. D., J. A. Oostveen, et al. (1998). "Relationship of microglial and astrocytic activation to disease onset and progression in a transgenic model of familial ALS." Glia **23**(3): 249-256.

He, T. C., S. Zhou, et al. (1998). "A simplified system for generating recombinant adenoviruses." Proc Natl Acad Sci U S A **95**(5): 2509-2514.

Henderson, C. E., E. Bloch-Gallego, et al. (1995). Purified embryonic motoneurons. Neural cell culture: A practical approach. J. Cohen and G. Wilkin. Oxoford, England, IRL Press**:** 69-81.

Henderson, C. E., W. Camu, et al. (1993). "Neurotrophins promote motor neuron survival and are present in embryonic limb bud." Nature **363**(6426): 266-270.

Henderson, C. E., H. S. Phillips, et al. (1994). "GDNF: a potent survival factor for motoneurons present in peripheral nerve and muscle." Science **266**(5187): 1062-1064.

Howland, D. S., J. Liu, et al. (2002). "Focal loss of the glutamate transporter EAAT2 in a transgenic rat model of SOD1 mutant-mediated

amyotrophic lateral sclerosis (ALS)." Proc Natl Acad Sci U S A **99**(3): 1604-1609.

Ischiropoulos, H., L. Zhu, et al. (1992). "Peroxynitrite-mediated tyrosine nitration catalyzed by superoxide dismutase." Archives of Biochemistry and Biophysics **298**(2): 431-437.

Jaarsma, D., E. Teuling, et al. (2008). "Neuron-Specific Expression of Mutant Superoxide Dismutase Is Sufficient to Induce Amyotrophic Lateral Sclerosis in Transgenic Mice." J. Neurosci. **28**(9): 2075-2088.

Jablonski, M. R., S. S. Markandaiah, et al. (2014). "Inhibiting drug efflux transporters improves efficacy of ALS therapeutics." Ann Clin Transl Neurol **1**(12): 996-1005.

Jean, Y. Y., L. D. Lercher, et al. (2008). "Glutamate elicits release of BDNF from basal forebrain astrocytes in a process dependent on metabotropic receptors and the PLC pathway." Neuron Glia Biol **4**(1): 35-42.

Jiang, B. H. and L. Z. Liu (2008). "PI3K/PTEN signaling in tumorigenesis and angiogenesis." Biochim Biophys Acta **1784**(1): 150-158.

Kang, S. H., Y. Li, et al. (2013). "Degeneration and impaired regeneration of gray matter oligodendrocytes in amyotrophic lateral sclerosis." Nat Neurosci **16**(5): 571-579.

Kastin, A. J., V. Akerstrom, et al. (2003). "Glial cell line-derived neurotrophic factor does not enter normal mouse brain." Neurosci Lett **340**(3): 239-241.

Kirby, J., K. Ning, et al. (2011). "Phosphatase and tensin homologue/protein kinase B pathway linked to motor neuron survival in human superoxide dismutase 1-related amyotrophic lateral sclerosis." Brain **134**(Pt 2): 506-517.

Lacomblez, L., G. Bensimon, et al. (1996). "Dose-ranging study of riluzole in amyotrophic lateral sclerosis. Amyotrophic Lateral Sclerosis/Riluzole Study Group II." Lancet **347**(9013): 1425-1431.

Lacomblez, L., G. Bensimon, et al. (1996). "A confirmatory dose-ranging study of riluzole in ALS. ALS/Riluzole Study Group-II." Neurology **47**(6 Suppl 4): S242-250.

Li, J. and J. Buchner (2013). "Structure, function and regulation of the hsp90 machinery." Biomed J **36**(3): 106-117.

Li, L., R. W. Oppenheim, et al. (1994). "Neurotrophic agents prevent motoneuron death following sciatic nerve section in the neonatal mouse." J Neurobiol **25**(7): 759-766.

Li, L., D. Prevette, et al. (1998). "Involvement of specific caspases in motoneuron cell death in vivo and in vitro following trophic factor deprivation." Mol Cell Neurosci **12**(3): 157-167.

Liao, B., W. Zhao, et al. (2012). "Transformation from a neuroprotective to a neurotoxic microglial phenotype in a mouse model of ALS." Exp Neurol **237**(1): 147-152.

Lyons, T. J., H. Liu, et al. (1996). "Mutations in copper-zinc superoxide dismutase that cause amyotrophic lateral sclerosis alter the zinc

binding site and the redox behavior of the protein." Proc Natl Acad Sci U S A **93**(22): 12240-12244.

Mahalingam, D., R. Swords, et al. (2009). "Targeting HSP90 for cancer therapy." Br J Cancer **100**(10): 1523-1529.

Martin, L. J., A. C. Price, et al. (2000). "Mechanisms for neuronal degeneration in amyotrophic lateral sclerosis and in models of motor neuron death (Review)." Int J Mol Med **5**(1): 3-13.

McCord, J. M. and I. Fridovich (1969). "Superoxide dimutase: an enzymic function for erythrocuprein (hemocuprein)." J Biol. Chem. **244**(22): 6049-6055.

Meininger, V., L. Lacomblez, et al. (2000). "What has changed with riluzole?" Journal of neurology **247 Suppl 6**: VI/19-22.

Milane, A., C. Fernandez, et al. (2010). "P-glycoprotein expression and function are increased in an animal model of amyotrophic lateral sclerosis." Neurosci Lett **472**(3): 166-170.

Milane, A., C. Fernandez, et al. (2007). "Minocycline and riluzole brain disposition: interactions with p-glycoprotein at the blood-brain barrier." J Neurochem **103**(1): 164-173.

Milane, A., S. Vautier, et al. (2009). "Interactions between riluzole and ABCG2/BCRP transporter." Neurosci Lett **452**(1): 12-16.

Miller, R. G., J. D. Mitchell, et al. (2012). "Riluzole for amyotrophic lateral sclerosis (ALS)/motor neuron disease (MND)." Cochrane Database Syst Rev **3**: CD001447.

Miller, R. G., D. H. Moore, 2nd, et al. (2001). "Phase III randomized trial of gabapentin in patients with amyotrophic lateral sclerosis." Neurology **56**(7): 843-848.

Milligan, C. E., D. Prevette, et al. (1995). "Peptide inhibitors of the ICE protease family arrest programmed cell death of motoneurons in vivo and in vitro." Neuron **15**(2): 385-393.

Miraglia, E., J. Hogberg, et al. (2012). "Statins exhibit anticancer effects through modifications of the pAkt signaling pathway." Int J Oncol **40**(3): 867-875.

Mistafa, O., A. Ghalali, et al. (2010). "Purinergic receptor-mediated rapid depletion of nuclear phosphorylated Akt depends on pleckstrin homology domain leucine-rich repeat phosphatase, calcineurin, protein phosphatase 2A, and PTEN phosphatases." J Biol Chem **285**(36): 27900-27910.

Mizuta, I., M. Ohta, et al. (2001). "Riluzole stimulates nerve growth factor, brain-derived neurotrophic factor and glial cell line-derived neurotrophic factor synthesis in cultured mouse astrocytes." Neuroscience letters **310**(2-3): 117-120.

Mojsilovic-Petrovic, J., N. Nedelsky, et al. (2009). "FOXO3a is broadly neuroprotective in vitro and in vivo against insults implicated in motor neuron diseases." J Neurosci **29**(25): 8236-8247.

Mollapour, M. and L. Neckers (2011). "Post-translational modifications of Hsp90 and their contributions to chaperone regulation." Biochimica et biophysica acta.

Mollapour, M., S. Tsutsumi, et al. (2010). "Swe1Wee1-dependent tyrosine phosphorylation of Hsp90 regulates distinct facets of chaperone function." Mol Cell **37**(3): 333-343.

Nagai, M., D. B. Re, et al. (2007). "Astrocytes expressing ALS-linked mutated SOD1 release factors selectively toxic to motor neurons." Nat Neurosci **10**(5): 615-622.

Nauser, T. and W. H. Koppenol (2002). "The rate constant of the reaction of superoxide with nitrogen monoxide: Approaching the diffusion limit." Journal of Physical Chemistry A **106**(16): 4084-4086.

Newbern, J., A. Taylor, et al. (2005). "Decreases in phosphoinositide-3-kinase/Akt and extracellular signal-regulated kinase 1/2 signaling activate components of spinal motoneuron death." Journal of Neurochemistry **94**(6): 1652-1665.

Ning, K., C. Drepper, et al. (2010). "PTEN depletion rescues axonal growth defect and improves survival in SMN-deficient motor neurons." Hum Mol Genet **19**(16): 3159-3168.

Nogradi, A., A. Szabo, et al. (2007). "Delayed riluzole treatment is able to rescue injured rat spinal motoneurons." Neuroscience **144**(2): 431-438.

Nogradi, A. and G. Vrbova (2001). "The effect of riluzole treatment in rats on the survival of injured adult and grafted embryonic motoneurons." Eur J Neurosci **13**(1): 113-118.

Oppenheim, R. W., Q. W. Yin, et al. (1992). "Brain-derived neurotrophic factor rescues developing avian motoneurons from cell death." Nature **360**(6406): 755-757.

Orrell, R. W. (2010). "Motor neuron disease: systematic reviews of treatment for ALS and SMA." British medical bulletin **93**: 145-159.

Padmaja, S. and R. E. Huie (1993). "The reaction of nitric oxide with organic peroxyl radicals." Biochem. Biophys. Res. Commun. **195**: 539-544.

Papadeas, S. T., S. E. Kraig, et al. (2011). "Astrocytes carrying the superoxide dismutase 1 (SOD1G93A) mutation induce wild-type motor neuron degeneration in vivo." Proc Natl Acad Sci U S A **108**(43): 17803-17808.

Pearl, L. H. and C. Prodromou (2000). "Structure and in vivo function of Hsp90." Current Opinion in Structural Biology **10**(1): 46-51.

Pearl, L. H. and C. Prodromou (2006). "STRUCTURE AND MECHANISM OF THE HSP90 MOLECULAR CHAPERONE MACHINERY." Annual Review of Biochemistry **75**(1): 271-294.

Pehar, M., P. Cassina, et al. (2004). "Astrocytic production of nerve growth factor in motor neuron apoptosis: implications for amyotrophic lateral sclerosis." J Neurochem **89**(2): 464-473.

Peluffo, H., A. G. Estévez, et al. (1997). "Riluzole promotes survival of rat motoneurons in vitro by stimulating trophic activity produced by spinal astrocyte monolayers." Neurosci Lett **228**(3): 207-211.

Pennica, D., V. Arce, et al. (1996). "Cardiotrophin-1, a cytokine present in embryonic muscle, supports long-term survival of spinal motoneurons." Neuron **17**(1): 63-74.

Pettmann, B. and C. E. Henderson (1998). "Neuronal cell death." Neuron **20**(4): 633-647.

Picard, D. (2002). "Heat-shock protein 90, a chaperone for folding and regulation." Cell Mol Life Sci **59**(10): 1640-1648.

Pratt, W. B., Y. Morishima, et al. (2008). "The Hsp90 Chaperone Machinery Regulates Signaling by Modulating Ligand Binding Clefts." J. Biol. Chem. **283**(34): 22885-22889.

Pratt, W. B. and D. O. Toft (2003). "Regulation of Signaling Protein Function and Trafficking by the hsp90/hsp70-Based Chaperone Machinery." Experimental Biology and Medicine **228**(2): 111-133.

Prodromou, C., S. M. Roe, et al. (1997). "Identification and structural characterization of the ATP/ADP-binding site in the Hsp90 molecular chaperone." Cell **90**(1): 65-75.

Rakhit, R., J. P. Crow, et al. (2004). "Monomeric Cu,Zn-superoxide dismutase is a common misfolding intermediate in the oxidation models of sporadic and familial amyotrophic lateral sclerosis." J Biol Chem **279**(15): 15499-15504.

Rao, R., W. Fiskus, et al. (2008). "HDAC6 inhibition enhances 17-AAG--mediated abrogation of hsp90 chaperone function in human leukemia cells." Blood **112**(5): 1886-1893.

Raoul, C., A. G. Estévez, et al. (2002). "Motoneuron death triggered by a specific pathway downstream of Fas: potentiation by ALS-linked SOD1 mutations." Neuron **35**: 1067-1083.

Raoul, C., C. E. Henderson, et al. (1999). "Programmed cell death of embryonic motoneurons triggered through the Fas death receptor." J Cell Biol **147**(5): 1049-1062.

Re, D. B., V. Le Verche, et al. (2014). "Necroptosis drives motor neuron death in models of both sporadic and familial ALS." Neuron **81**(5): 1001-1008.

Reaume AG, E. J., Hoffman EK, Kowall NW, Ferrante RJ, Siwek DF, Wilcox HM, Flood DG, Beal MF, Brown RH Jr, Scott RW, Snider WD. (1996). "Motor neurons in Cu/Zn superoxide dismutase-deficient mice develop normally but exhibit enhanced cell death after axonal injury." Nat Genet **13**(1): 43-47.

Reaume, A. G., J. L. Elliott, et al. (1996). "Motor neurons in Cu/Zn superoxide dimutase-deficient mice develop normally but exhibit enhanced cell death after axonal injury." Nature Genetics **13**: 43-47.

Richter, K. and J. Buchner (2001). "Hsp90: chaperoning signal transduction." J Cellular Physiol. **188**(3): 281-290.

Richter, K., M. Haslbeck, et al. (2010). "The heat shock response: life on the verge of death." Mol Cell **40**(2): 253-266.

Robinson, M. B., D. J. Gifondorwa, et al. (2010). Mechanisms of the Motoneuron Stress Response and Its Relevance in Neurodegeneration. Neurodegeneration: Theory, Disorders and Treatments. A. S. McNeill, Nova Science Publishers, Inc.

Robinson, M. B., J. L. Tidwell, et al. (2005). "Extracellular Heat Shock Protein 70: A Critical Component for Motoneuron Survival." J. Neurosci. **25**(42): 9735-9745.

Rosen, D. R., T. Siddique, et al. (1993). "Mutations in Cu/Zn superoxide dimutase gene are associated with familial amyotrophic lateral sclerosis." Nature **362**(6415): 59-62.

Rossi, F. H., M. C. Franco, et al. (2013). Pathophysiology of Amyotrophic Lateral Sclerosis. Rejeka, Croatia, InTech.

Rothstein, J. D. and R. W. Kuncl (1995). "Neuroprotective strategies in a model of chronic glutamate-mediated motor neuron toxicity." J Neurochem **65**(2): 643-651.

Rotunno, M. S. and D. A. Bosco (2013). "An emerging role for misfolded wild-type SOD1 in sporadic ALS pathogenesis." Front Cell Neurosci **7**: 253.

Rumfeldt, J. A., J. R. Lepock, et al. (2009). "Unfolding and folding kinetics of amyotrophic lateral sclerosis-associated mutant Cu,Zn superoxide dismutases." J Mol Biol **385**(1): 278-298.

Rumfeldt, J. A., P. B. Stathopulos, et al. (2006). "Mechanism and thermodynamics of guanidinium chloride-induced denaturation of ALS-associated mutant Cu,Zn superoxide dismutases." J Mol Biol **355**(1): 106-123.

Sahawneh, M. A., K. C. Ricart, et al. (2010). "Cu,Zn superoxide dismutase (SOD) increases toxicity of mutant and Zn-deficient superoxide dismutase by enhancing protein stability." J Biol Chem **285**(44): 33885-33897.

Saneto, R. P. and J. D. Vellis (1987). Neuronal and glial cells: cell culture of the central nervous system. Neurochemistry a practical approach. A. J. Turner and H. S. Brachelard. Washington, D.C., IRL Press Oxford**:** 27-63.

Sato, S., N. Fujita, et al. (2000). "Modulation of Akt kinase activity by binding to Hsp90." PNAS **97**(20): 10832-10837.

Sato, T., Nakanishi, T., Yamamoto, Y., Andersen, PM, Ogawa, Y, Fukada, K, Zhou, Z, Aoike, F., Sugai, F., Nagano, S., Hirata, S., Ogawa, M., Nakano, R., Ohi, T., Kato, T., Nakagawa, M., Hamasaki, T., Shimizu, A., and Sakoda, S. (2005). "Rapid disease progression correlates with instability of mutant SOD1 in familial ALS." Neurology **65**(12): 1954-1957.

Schaar, D. G., B. A. Sieber, et al. (1993). "Regional and cell-specific expression of GDNF in rat brain." Exp Neurol **124**(2): 368-371.

Schiffer, D., S. Cordera, et al. (1996). "Reactive astrogliosis of the spinal cord in amyotrophic lateral sclerosis." J Neurol Sci **139**: 27-33.

Schnaar, R. I. and A. E. Schaffner (1981). "Separation of cell types from embryonic chicken and rat spinal cord: characterization of motoneuron-enriched fractions." J Neurosci **1**(2): 204-217.

Sendtner, M., Y. Arakawa, et al. (1991). "Effect of ciliary neurotrophic factor (CNTF) on motoneuron survival." J Cell Sci Suppl **15**: 103-109.

Shinder, G., Lacourse, M., Minotti, S., and Durham, HD (2001). "Mutant Cu/Zn-Superoxide Dismutase Proteins Have Altered Solubility and Interact with Heat Shock/Stress Proteins in Models of Amyotrophic Lateral Sclerosis." Journal of Biological Chemistry **276**(16): 12791-12796.

Soler, R. M., X. Dolcet, et al. (1999). "Receptors of the glial cell line-derived neurotrophic factor family of neurotrophic factors signal cell survival through the phosphatidylinositol 3-kinase pathway in spinal cord motoneurons." J Neurosci **19**(21): 9160-9169.

Spear, N., A. G. Estévez, et al. (1997). Peroxynitrite and Cell signalling. Oxidative Stress and Signal Transduction. H. J. Forman and E. Cadenas. New york, Chapman&Hall**:** 32-51.

Stebbins, C. E., A. A. Russo, et al. (1997). "Crystal structure of an Hsp90-geldanamycin complex: targeting of a protein chaperone by an antitumor agent." Cell **89**(2): 239-250.

Subramaniam, J. R., W. E. Lyons, et al. (2002). "Mutant SOD1 causes motor neuron disease independent of copper chaperone-mediated copper loading." Nature Neurosci **5**(4): 301-307.

Tang, E. D., G. Nunez, et al. (1999). "Negative regulation of the forkhead transcription factor FKHR by Akt." J Biol Chem **274**(24): 16741-16746.

Taylor, A. R., D. J. Gifondorwa, et al. (2007). "Astrocyte and Muscle-Derived Secreted Factors Differentially Regulate Motoneuron Survival." J. Neurosci. **27**(3): 634-644.

Thaxton, C., M. Bott, et al. (2011). "Schwannomin/merlin promotes Schwann cell elongation and influences myelin segment length." Mol Cell Neurosci **47**(1): 1-9.

Vinsant, S., C. Mansfield, et al. (2013). "Characterization of early pathogenesis in the SOD1(G93A) mouse model of ALS: part I, background and methods." Brain Behav **3**(4): 335-350.

Vinsant, S., C. Mansfield, et al. (2013). "Characterization of early pathogenesis in the SOD1(G93A) mouse model of ALS: part II, results and discussion." Brain Behav **3**(4): 431-457.

Vucic, S., C. S. Lin, et al. (2013). "Riluzole exerts central and peripheral modulating effects in amyotrophic lateral sclerosis." Brain **136**(Pt 5): 1361-1370.

Walton-Diaz, A., S. Khan, et al. (2013). "Contributions of co-chaperones and post-translational modifications towards Hsp90 drug sensitivity." Future Med Chem **5**(9): 1059-1071.

Wang, J. J., H. H. Slunt, et al. (2003). "Copper-binding-site-null SOD1 causes ALS in transgenic mice: aggregates of non-native SOD1 delineate a common feature." Human molecular genetics **12**(21): 2753.

Wang, L., H. X. Deng, et al. (2009). "Wild-type SOD1 overexpression accelerates disease onset of a G85R SOD1 mouse." Hum Mol Genet **18**(9): 1642-1651.

Wang, L., K. Sharma, et al. (2008). "Restricted expression of mutant SOD1 in spinal motor neurons and interneurons induces motor neuron pathology." Neurobiol Dis **29**(3): 400-408.

Weng, L., J. Brown, et al. (2001). "PTEN induces apoptosis and cell cycle arrest through phosphoinositol-3-kinase/Akt-dependent and -independent pathways." Hum Mol Genet **10**(3): 237-242.

Whitesell, L. and S. L. Lindquist (2005). "Hsp90 and the chaperoning of cancer." Nature Reviews Cancer **5**(10): 761-772.

Wilhelm, J. C., M. Xu, et al. (2012). "Cooperative roles of BDNF expression in neurons and Schwann cells are modulated by exercise to facilitate nerve regeneration." J Neurosci **32**(14): 5002-5009.

Wong, P. C., H. Cai, et al. (2002). "Genetically engineered mouse models of neurodegenerative diseases." Nat Neurosci **5**(7): 633-639.

Wong, P. C., C. A. Pardo, et al. (1995). "An Adverse Property of a Familial Als-Linked Sod1 Mutation Causes Motor-Neuron Disease Characterized by Vacuolar Degeneration of Mitochondria." Neuron **14**(6): 1105-1116.

Xiao, N., C. W. Callaway, et al. (1999). "Geldanamycin Provides Posttreatment Protection Against Glutamate-Induced Oxidative

Toxicity in a Mouse Hippocampal Cell Line." Journal of Neurochemistry **72**(1): 95-101.

Xu, P., K. M. Rosen, et al. (2013). "Nerve injury induces glial cell line-derived neurotrophic factor (GDNF) expression in Schwann cells through purinergic signaling and the PKC-PKD pathway." Glia **61**(7): 1029-1040.

Yamanaka, K., S. J. Chun, et al. (2008). "Astrocytes as determinants of disease progression in inherited amyotrophic lateral sclerosis." Nat Neurosci **11**(3): 251-253.

Yang, D. J., X. L. Wang, et al. (2014). "PTEN regulates AMPA receptor-mediated cell viability in iPS-derived motor neurons." Cell Death Dis **5**: e1096.

Ye, Y., C. Quijano, et al. (2007). "Prevention of peroxynitrite-induced apoptosis of motor neurons and PC12 cells by tyrosine-containing peptides." J. Biol. Chem. **282**: 6324-6337.

Zhao, R., M. Davey, et al. (2005). "Navigating the Chaperone Network: An Integrative Map of Physical and Genetic Interactions Mediated by the Hsp90 Chaperone." Cell **120**(5): 715-727.